RESEARCH ARTICLE

The receptor-like kinase BIR1 inhibits elicitor-induced plasmodesmata callose deposition and PTI gene expression and requires EDS1 and SOBIR1 to cause dose-dependent cell-death in Arabidopsis

Irene Guzmán-Benito[1], Carmen Robinson[1,2], Chenlei Hua[3], Ana Rocio Sede[4], Laura Elvira-González[4], Isabel Punzón[1], Manfred Heinlein[4], Thorsten Nürnberger[3,5], César Llave[1]*

[1]Centro de Investigaciones Biológicas Margarita Salas. Consejo Superior de Investigaciones Científicas, Ramiro de Maeztu 9, 28040 Madrid, Spain; [2]Doctorado en Biotecnología y Recursos Genéticos de Plantas y Microorganismos Asociados, Universidad Politécnica de Madrid, 28040-Madrid, Spain; [3]Department of Plant Biochemistry, Center of Plant Molecular Biology (ZMBP), University of Tübingen, Tübingen, Germany; [4]Institut de Biologie Moléculaire des Plantes, CNRS, Université de Strasbourg, 67000 Strasbourg, France; [5]Department of Biochemistry, University of Johannesburg, Johannesburg, South Africa.

Author for correspondence: *César Llave*

E-mail: cesarllave@cib.csic.es

Phone: +34-91-8373112

WORD COUNT: 6457

Summary: 197

Introduction: 924

Materials and methods: 356

Results: 3532

Discussion: 1581

Acknowledgments: 64

Number of figures: 7

Number of figures in color: 7

Supporting information

Number of supporting methods: 3

Number of supporting figures: 8

Number of supporting tables: 8

ORCIDS

Irene Guzmán-Benito	0000-0002-9912-8164
Carmen Robinson	0000-0002-7146-0253
Chenlei Hua	0000-0002-6630-9049
Ana Rocio Sede	0000-0002-7868-0638
Laura Elvira-González	0000-0002-2530-8912
Manfred Heinlein	0000-0001-7322-1654
Thorsten Nürnberger	0000-0002-7804-7170
César Llave	0000-0003-3844-4582

Summary

- The receptor-like kinase BAK1-INTERACTING RECEPTOR-LIKE KINASE 1 (BIR1) functions as a negative regulator of cell death and defense in Arabidopsis. Previous studies showed that BIR1 expression is up-regulated during infections with microbes and viruses. However, the biological consequences of BIR1 induction remain unknown.
- Here, we use a dexamethasone (DEX)-inducible expression system in *Arabidopsis thaliana* to investigate the outputs associated with physiological and non-physiological levels of BIR1 expression.
- We show that BIR1 induction at physiological levels significantly interferes with gene expression and plasmodesmata callose deposition triggered by canonical pattern-triggered immunity (PTI) elicitors. Plants that accumulated non-physiological doses of BIR1 displayed morphological defects that concur with transcriptomic changes in multiple plant defense genes. We provide experimental evidence that ENHANCED DISEASE SUSCEPTIBILITY 1 (EDS1) and SUPPRESSOR OF BIR1-1 (SOBIR1) are required for the effector-triggered immunity (ETI)-type cell death phenotypes associated with non-physiological levels of BIR1
- We propose that BIR1 induction may represent a pathogen-triggered mechanism to modulate plant defenses during infection. Our model predicts that when BIR1 regulation is lost, BIR1 integrity is sensed by one or several guarding resistance (R) proteins to initiate an ETI-like response, in which SOBIR1 cooperates with EDS1 to transduce signals downstream of R proteins.

Key words

Arabidopsis, BAK1-INTERACTING RECEPTOR-LIKE KINASE 1 (BIR1), cell death, ENHANCED DISEASE SUSCEPTIBILITY 1 (EDS1), immune regulation, immune receptor, pattern-triggered immunity, SUPPRESSOR OF BIR1 (SOBIR1)

Introduction

Plants use immunity to defend themselves against invaders such as bacteria, fungi, oomycetes, and viruses (Korner *et al.*, 2013; Nishad *et al.*, 2020). Pattern-triggered immunity (PTI) uses multiple cell-surface pattern recognition receptors (PRR) to recognize pathogen/microbe/damage-associated molecular patterns (PAMP/MAMP/DAMP). Effector-triggered immunity (ETI) involves intracellular receptors that sense pathogen-effector proteins or effector-induced manipulations of host proteins (Zhou & Zhang, 2020; Yu *et al.*, 2021). PRRs are single-transmembrane receptor-like kinases (RLK) or receptor-like proteins (RLP). PRRs form active receptor complexes in a ligand-dependent manner with members of the somatic embryogenesis co-receptor kinases (SERKs), including BRASSINOSTEROID INSENSITIVE1-ASSOCIATED RECEPTOR KINASE 1 (BAK1/SERK3) (Boutrot & Zipfel, 2017; Hohmann *et al.*, 2017; Smakowska-Luzan *et al.*, 2018). BAK1 functions as a positive regulator of PTI (Wu *et al.*, 2020), and has a dual role as positive and negative regulator of cell death during ETI (Belkhadir *et al.*, 2012; Dominguez-Ferreras *et al.*, 2015). RLP-type PRRs lack kinase activity and constitutively associate in a ligand-independent manner with the leucine-rich repeat (LRR)-RLK SUPPRESSOR OF BIR1-1 (SOBIR1) (Gust *et al.*, 2017). Once the microbe is sensed, PRR complexes activate receptor-like cytoplasmic kinases (RLCKs) that initiate downstream signaling cascades (Liang & Zhou, 2018; Rao *et al.*, 2018). Among them, BOTRYTIS INDUCED KINASE1 (BIK1) functions as a positive regulator of immunity when triggered by LRR-RLKs or as a negative regulator when triggered by LRR-RLPs (Bi *et al.*, 2018; Wan *et al.*, 2019).

ETI relies on nucleotide-binding domain LRR intracellular immune receptors (NLRs) encoded by polymorphic disease resistance genes (R). NLRs comprise either proteins with an N-terminal domain similar to the TOLL/INTERLEUKIN RECEPTOR 1 (TIR1) (TIR-NB-LRR, TNL), proteins with a coiled-coil (CC) domain at the N terminus (CC-NB-LRR, CNL) or proteins with a RESISTANCE TO POWDERY MILDEW 8-LIKE DOMAIN (RPW8)-type domain (RNLs) (van Wersch *et al.*, 2020; Wang & Chai, 2020). NLRs function as “sensors” that recognize effectors, or as “helpers” that mediate signaling downstream of sensor NLRs (Jubic *et al.*, 2019). Recent studies demonstrated that PTI and ETI work together to mutually potentiate the immune response (Yuan *et al.*, 2021b; Yuan *et al.*, 2023). NLR-mediated signaling is dependent on multiple PTI-associated components such as BAK1, SOBIR1, or BIK1 in a PTI-independent manner, while TNL genes that are up-regulated during early PTI boost immune responses (Ngou *et al.*, 2021; Tian *et al.*, 2021; Yuan *et al.*, 2021a). ENHANCED

109 DISEASE SUSCEPTIBILITY (EDS1) and PHYTOALEXIN DEFICIENT 4 (PAD4), which
110 are essential in TNL-mediated immunity, also play a key role in PTI signaling in response to
111 different microbial elicitors (Pruitt *et al.*, 2021b; Tian *et al.*, 2021). Furthermore, PTI and ETI
112 outputs usually converge, albeit with different amplitude and duration (Yuan *et al.*, 2021b).
113 Early immune responses include apoplastic reactive oxygen species (ROS) burst, cytosolic
114 calcium (Ca^{+2}) influx and activation of Ca^{+2}-dependent protein kinases (CPK), and activation
115 of mitogen-activated protein kinases (MAPK). This response is followed by the transcriptional
116 activation of defense processes that include accumulation of defense phytohormones, regulation
117 of cell wall and secretome composition (Li *et al.*, 2020).

118 Plants deploy a variety of mechanisms to avoid the detrimental effects of hyperactivated
119 defenses (Couto & Zipfel, 2016; Withers & Dong, 2017; Mithoe & Menke, 2018). BAK1-
120 INTERACTING RECEPTOR-LIKE KINASE (BIR) proteins play a key role in defense
121 attenuation. The current model postulates that, in the absence of microbes, BIR proteins
122 constitutively associate with BAK1, maintaining the PRRs in a resting state. During ligand
123 perception, BAK1 dissociates from BIR and becomes accessible to complex with PRR
124 receptors (Gao *et al.*, 2009; Halter *et al.*, 2014; Imkampe *et al.*, 2017). The Arabidopsis genome
125 contains four BIR homologs. Arabidopsis BIR1 negatively regulates cell death signaling
126 pathways that depend on BAK1, SOBIR1, EDS1 and PAD4, and that likely involve
127 components of the TNL-mediated ETI response (Gao *et al.*, 2009; Schulze *et al.*, 2022).
128 Arabidopsis BIR2 and BIR3 have critical roles in the negative regulation of the PRR-mediated
129 PTI response (Halter *et al.*, 2014; Imkampe *et al.*, 2017). BIR4 has so far not been characterized.

130 Under normal conditions, BIR1 expression is transcriptionally activated by multiple
131 microbial and viral pathogens in a salicylic acid (SA)-dependent manner (Guzman-Benito *et*
132 *al.*, 2019). RNA-directed DNA methylation and post-transcriptional RNA silencing maintain
133 BIR1 transcripts at physiological levels when BIR1 is actively transcribed (Guzman-Benito *et*
134 *al.*, 2019). However, transgenic overexpression of BIR1 at non-physiological levels triggers
135 developmental defects and cell death similar to the autoimmune phenotypes observed in *bir1-*
136 *1* mutants (Gao *et al.*, 2009; Guzman-Benito *et al.*, 2019). Given that perturbations in BIR1
137 homeostasis have severe growth-defense penalties, effective strategies for BIR1 regulation are
138 needed to prevent unbearably high levels of BIR1 expression. To date, the effects and
139 importance of BIR1 induction in plant defense remain largely unknown.

140 In this work, we conducted a time-course analysis of the phenotypical outputs associated
141 with physiological and non-physiological levels of BIR1 expression in Arabidopsis. We first

142 tested if BIR induction interferes with the immune response triggered by canonical PAMPs.
143 We found that physiological induction of BIR1 represses the expression of PTI genes and
144 plasmodesmata (PD) callose deposition in response to several PTI elicitors. Whereas
145 physiological induction of BIR1 has a subtle impact on the plant transcriptome, the
146 morphological and growth defects caused when BIR1 is expressed at non-physiological levels
147 are concomitant with the transcriptional reprogramming of multiple genes encoding
148 components of PTI and ETI pathways. We found that the cell death phenotypes associated with
149 BIR1 overexpression require the TNL-associated EDS1 and/or the RLP-co-receptor SOBIR1,
150 but the underlying mechanism is unknown. Finally, our work demonstrates that a well-balanced
151 expression of BIR1 avoids interference with cellular processes of growth and development, and
152 is critical for plant fitness.

153

154 **Material and Methods**

155 **Plant material and growth condition**

156 *Arabidopsis thaliana* plants were grown in controlled environmental chambers under long-day
157 conditions (16h day/8h night) at 22°C. Arabidopsis lines used in this study were derived from
158 the Columbia-0 (Col-0) ecotype. Seeds were surface-sterilized and sown on plates containing
159 ½ Murashige and Skoog (MS) medium supplemented with MES (0,5g/L), 1% sucrose and 0,9%
160 Plant agar (Duchefa Biochemie). Seedlings were transferred to soil 7 to 10 days after
161 germination.

162 Mutants for *bir1-1* and *sobir1-12* were donated by Yuelin Zhang (University of British
163 Columbia, Canada). The Arabidopsis *eds1-2*, *pad4-1* and *eds5-3* alleles were supplied by Jane
164 E. Parker (Max Planck Institute for Plant Breeding Research, Germany). Arabidopsis mutant
165 *bak1-5* was donated by Birgit Kemmerling (Center of Plant Molecular Biology, University of
166 Tübingen, Germany). The *sid2-2* mutant was a gift from Francisco Tenllado (Centro de
167 Investigaciones Biológicas Margarita Salas, CSIC, Spain).

168 Arabidopsis Col-0 transgenic plants expressing a BIR1-mCherry fusion under a
169 dexamethasone (DEX)-inducible gene expression system (BIR1 L6 and BIR1 L9) have already
170 been described (Guzman-Benito *et al.*, 2019). In this study, the same DEX-inducible expression
171 system containing a mCherry-tagged BIR1 (hereafter BIR1) protein-coding gene was
172 transformed into Arabidopsis mutant backgrounds according to standard floral dipping (Clough
173 & Bent, 1998). Independent homozygous lines were selected in T3 and used for subsequent

experiments. Morphological phenotypes after DEX treatments were investigated in two independent transgenic lines of each genotype.

Protein and RNA analyses

Protein assays and one-step quantitative RT-PCR (RT-qPCR) using gene-specific primers (Table S1) and CBP20 (At5g44200) as endogenous reference gene are described in Methods S1.

Library preparation for transcriptome sequencing and bioinformatic analyses

A total of 24 samples, including three biological replicates per treatment, were collected for RNA-Seq. Each sample consisted of RNA pooled from six individual plants. Sequencing libraries, transcriptome sequencing of paired-end reads using an Illumina PE150 Hiseq platform and bioinformatic analyses were done at NOVOGENE (HK) COMPANY LIMITED (Wan Chai, Hong Kong) as described (Methods S2). The raw data was deposited in the Gene Expression Omnibus under accession number GSE234036.

Analyses of Reactive oxygen species (ROS) and ethylene, plasmodesmata callose deposition and dexamethasone (DEX) treatments.

Experimental procedures are described in Methods S3.

Results

BIR1 induction causes dose-dependent transcriptome reprogramming in Arabidopsis

We conducted a RNA-Seq assay on Arabidopsis BIR1 L9 plants, which express a DEX-inducible BIR1-mCherry transgene (Guzman-Benito *et al.*, 2019), to understand the downstream biological processes and pathways associated with BIR1 induction, This system proved to be a valuable tool for studying BIR1 effects in the absence of pathogen elicitors or effectors. Three-week-old plants were sprayed with a 30 µM DEX solution at 24 h intervals and rosette leaf samples were harvested for next-generation sequencing. Control plants were mock-treated with H_2O. Three biological replicates were used as representative samples of each condition tested in this study: DEX-treated WT (DeWT_), mock-treated WT (MoWT_), DEX-treated BIR1 L9 (DeL9_) and mock-treated BIR1 L9 (MoL9_) plants at 4 or 12 days of treatment as indicated **(Table S2)**. After four days of DEX treatment, BIR1 L9 plants developed normally like WT plants, but they started showing a range of morphological and growth defects from day 12 onward, including stunting, leaf deformation, premature senescence (yellowing),

205 and cell-death **(Fig. 1a)**. To avoid extensive damage on the plant transcriptome, DeL9_ samples
206 were collected before the onset of cell death symptoms. DeL9_ samples accumulated BIR1 at
207 physiological levels after 4 days of DEX treatment whereas non-physiological levels of BIR1
208 occurred after long BIR1 induction periods (12 days of DEX treatment) **(Fig. 1a)**. (Guzman-
209 Benito *et al.*, 2019).

210 Principal component analysis (PCA) was used to sort RNA-seq-based transcriptomic data
211 according to gene expression levels. To discard the potential effects of DEX on gene expression,
212 we first compared DEX-treated WT versus DEX-treated BIR1 L9 plants. PC1 defined a distinct
213 separation in the PCA score plot between WT (DeWT_12) and BIR1 L9 (DeL9_12) samples
214 after 12 days of treatment, indicating that the BIR1 expression level was the main source of
215 variance (36.92%) **(Fig. 1b)**. Samples in the DeL9_4 group, which produced physiological
216 levels of BIR1, clustered in the proximity of non-transgenic DeWT_4 samples, reflecting their
217 similar expression profiles. PC2 seems to highlight a shift in gene expression between samples
218 due to age or developmental stage (22.07%). When DEX-treated BIR1 L9 plants were
219 compared with mock-treated BIR1 L9 plants, the BIR1 expression level was again the dominant
220 source of variance (36.85%) underlying PC1, whereas time was the basis for PC2 (19.57%)
221 separation in the PCA score plot **(Fig. S1a)**. BIR1 abundance [measured in Fragments Per
222 Kilobase of transcript sequence per Millions of base-pairs sequenced (FPKM)] in replicate
223 DeL9_12b was substantially lower than in the other two DeL9_12 replicates within the
224 DeL9_12 group **(Fig. 1a**). Interestingly, the DeL9_12b sample was located far from the other
225 DeL9_12 samples in the PCA plot, and was found near the samples within the DeWT_12 or
226 MoL9_12 clusters **(Figs. 1b, S1a)**. This finding may suggest that moderate BIR1
227 overexpression produced less transcriptomic alterations than high BIR1 overexpression levels
228 relative to the controls.

229 Differentially expressed genes (DEG) from different comparisons are presented in **Table**
230 **S3**. Our data indicate that a massive transcriptional reprogramming occurs when BIR1 is
231 overexpressed in Arabidopsis (12 days of DEX treatment) but not when BIR1 is
232 transcriptionally induced at physiological levels (4 days of DEX treatment) **(Fig. 1c)** (**Table**
233 **S4)**. DEGs using different statistical thresholds are shown in **Figs. S1b,c**. Gene ontology (GO)
234 analysis showed that genes encoding proteins with oxidoreductase activity, transmembrane
235 transport and other metabolic processes or genes related to lipid or carbohydrate metabolism
236 were particularly overrepresented in our whole set of DEGs, including WT and BIR1 L9 plants
237 **(Figs. 1d, S1d, S2d) (Table S5)**. These alterations presumably reflect the effects of DEX on

238 the plant transcriptome. However, DEGs with kinase activity were only enriched in BIR1
239 overexpressing plants, relative to mock-treated BIR1 L9 plants **(Figs. 1d, S1d)** or DEX-treated
240 WT plants **(Fig. S2d),** ruling out an effect caused by DEX. The Kyoto Encyclopedia of Genes
241 and Genomes (KEGG) pathway analysis showed the enrichment of genes related to several
242 metabolic processes and genes involved in the biosynthesis of secondary metabolites that were
243 specifically activated after DEX-treatments **(Fig. S3) (Table S6)**. Conversely, DEGs involved
244 in plant hormone signal transduction were significantly enriched only in DEX-treated BIR1 L9,
245 but not in mock-treated BIR1 L9 plants or DEX-treated WT plants. The impact of DEX
246 application on plant morphology and gene expression in WT plants is shown in **Fig. S2** and
247 **Table S4**.

248

249 **Effects of BIR1 induction on PTI activation in response to bacterial elicitors**

250 We assessed the effects of inducing BIR1 at physiological levels on the early events of PTI
251 response. BIR1 was induced by treating BIR1 transgenic plants (L6 and L9) with a 30 µM DEX
252 solution 4 times at 24 h intervals, whereas control plants were mock-treated with H_2O. The
253 flg22 peptide derived from bacterial flagellin and the nlp20 fragment of NECROSIS AND
254 ETHYLENE-INDUCING PEPTIDE 1 (NEP1)-LIKE proteins (NLP) were used as elicitors.
255 The luminol-based assay showed that ROS production triggered by 1 µM flg22 or nlp20 was
256 comparable between WT, BIR1 L6 and BIR1 L9 plants **(Fig. 2a**). Likewise, production of the
257 phytohormone ethylene was similarly increased in DEX-treated WT, BIR1 L6 and BIR1 L9
258 plants in response to flg22 and, to a greater extent, in response to nlp20 at concentrations of 1
259 µM and 100 nM. These findings indicate that induction of BIR1 had no measurable effects on
260 ROS and ethylene accumulation triggered by canonical elicitors **(Fig. 2b)**. Next, we tested the
261 expression of genes encoding the canonical PTI markers FLG22-INDUCED RECEPTOR-
262 LIKE KINASE 1 (FRK1) and PATHOGENESIS RELATED 1 (PR1) in BIR1 L6 and BIR1 L9
263 transgenic plants upon 1 µM flg22 elicitation. Whereas all these genes were significantly up-
264 regulated in mock-treated controls, they were no longer activated upon BIR1 induction in DEX-
265 treated BIR1 L6 an BIR1 L9 plants. Both PTI markers were altered by flg22 in WT plants
266 treated with DEX, which discarded a potential repressive effect of DEX on PTI gene expression
267 **(Fig. 2c)**. The induction of BIR1 protein in the BIR1 L6 and BIR1 L9 plants used for ROS and
268 ethylene assays was confirmed by immunocapture followed by western blot, while BIR1
269 transcripts were monitored in the samples used for RT-qPCR expression assays (**Fig. 2d**).

270 Collectively, these results indicate that BIR1 induction at physiological levels negligibly
271 affects ROS production and ethylene accumulation but interferes with downstream events of
272 the PTI pathway, impacting the transcriptional activation of defense genes.

273

274 **Induction of BIR1 hinders callose deposition at PD triggered by flg22 or dsRNA**

275 During the early stages of pathogen invasion, conserved PAMPs trigger callose depositions in
276 the cell-wall and PD (Luna *et al.*, 2011). Deposition of callose at PD regulates symplastic
277 transport, and limits the ability of the invading pathogen to enter plant tissues (Tang *et al.*, 2017;
278 Huang *et al.*, 2023). To investigate whether BIR1 induced at physiological levels affects callose
279 deposition in PD, we used *in vivo* aniline blue staining to quantify PD-associated callose from
280 digital photographs of BIR1 L9 Arabidopsis plants. BIR1 was induced with a 30 µM DEX
281 solution 3 times at 24h intervals, whereas control plants were mock-treated with H_2O. We first
282 investigated callose deposition using 1 µM flg22 as elicitor. Compared to plants treated without
283 the elicitor (H_2O), flg22 caused a noticeable increase in PD callose intensity BIR1 L9 control
284 plants (DEX-) **(Figs. 3a,c)**. In contrast, PD-associated callose was no longer induced by flg22
285 in plants expressing the BIR1 transgene (DEX+) **(Figs. 3a,c)**. BIR1 L9 plants were later treated
286 with the synthetic dsRNA analog polyinosinic-polycytidylic acid [poly(I:C)] (0.5 µg μl^{-1}) as
287 dsRNA is known to trigger deposition of callose and PD closure in Arabidopsis (Huang *et al.*,
288 2023). In the absence of DEX, callose intensity was significantly higher in BIR1 L9 plants
289 treated with poly(I:C) compared to H_2O-treated plants. In contrast, after DEX treatment,
290 poly(I:C)-induced callose was significantly repressed by the expression of BIR1 (**Figs. 3b,c)**.
291 We observed enhanced callose deposition in WT controls and DEX-treated WT plants in
292 response to flg22 and poly(I:C) relative to H_2O-treated plants, suggesting that DEX does not
293 affect callose deposition **(Fig. 3d)**. These findings indicate that the induction of BIR1 impairs,
294 at least partially, PD callose deposition triggered by different PAMP elicitors.

295

296 **BIR1 overexpression triggers the expression of immunity-related genes**

297 RNA-Seq results were further validated in mock- and DEX-treated BIR1 L9 plants after 12
298 days of treatment using RT-qPCR. We found that expression of DEGs encoding BIR1, PR1,
299 RESPIRATORY BURST OXIDASE HOMOLOG PROTEIN D (RBOHD), FRK1 and
300 CYTOCHROME P450 MONOOXYGENASE 79B2 (CYP79B2) defense markers were all up-
301 regulated in Arabidopsis plants overexpressing BIR1 compared to mock-treated controls, which

302 is consistent with their RNA-Seq-based profiles and confirms reproducibility in their expression
303 patterns **(Fig. 4a)**.

304 A detailed inspection of the RNA-Seq data revealed that multiple genes involved in the
305 perception of pathogens and the activation of defense pathways were misregulated when BIR1
306 was overexpressed [$|\log_2$ (Fold-Change)$| \geq 1$ and adjusted *p*-value ≤ 0.01] **(Table S7, S8)**. Two-
307 tailed Fisher's exact tests revealed that genes encoding LRR-type RLKs in the Arabidopsis
308 genome were significantly enriched **(Table S7)**. Cysteine-rich RLKs (CRK), which are
309 important in the perception of apoplastic ROS and, likely in association with BAK1, in the
310 activation of PTI and cell death, were overrepresented in the pool of DEGs **(Table S7) (Fig.
311 S4)** (Chen, 2001)(Yeh *et al.*, 2015; Quezada *et al.*, 2019; Castro *et al.*, 2021). Furthermore, a
312 significant percentage of RLP coding genes in Arabidopsis were in the list of DEGs **(Tables
313 S7) (Fig. S5)** (Wang *et al.*, 2008; Lv *et al.*, 2016). Most of LRR-RLK, CRK and RLP transcripts
314 were up-regulated in response to elevated BIR1, but not in DEX-treated WT plants. BIR1
315 overexpression boosted the transcription of many other genes involved in PTI and ETI signaling
316 **(Figs. 4b, S6)**. This includes the RLK co-receptors BAK1 and SOBIR1, RLCKs such as BIK1
317 and several AvrPphB SUSCEPTIBLE1(PBS1)-LIKE (PBL) kinases (PBL4, PBL12, PBL20)
318 (Liang & Zhou, 2018; Rao *et al.*, 2018) **(Table S7)**. Active BIK1 positively regulates the Ca^{2+}
319 influx from the apoplast to the cytosol, which switches on the kinase activity of CPKs (Li *et
320 al.*, 2014; Yip Delormel & Boudsocq, 2019). Collectively, CPKs were not differentially
321 regulated, but many individual CPKs were regarded as DEGs in plants overexpressing BIR1
322 (Table S3). For instance, the expression of CPK4-6 and CPK11, which are key players in
323 transcriptional reprogramming upon elicitor perception, was enhanced only in DEX-treated
324 BIR1 L9 plants **(Fig. S7a)** (Boudsocq *et al.*, 2010). Upon ligand perception, BIK1 dissociates
325 from activated receptor complexes and phosphorylates the plasma membrane NADPH oxidase
326 RBOHD to generate extracellular ROS (Kadota *et al.*, 2014; Li *et al.*, 2014). Interestingly,
327 RBOHD was induced in DEX-treated BIR1 L9 plants after both 4 and 12 days of treatment, but
328 not in their corresponding controls **(Figs. 4a,b)**. Genes encoding the lipase-like proteins EDS1,
329 PAD4, SENESCENCE ASSOCIATED-GENE 101 (SAG101) and ACTIVATED DISEASE
330 RESISTANCE 1 (ADR1), which are required for TNL-receptor function during ETI, were also
331 up-regulated (Table S3) **(Fig. 4b)** (Zhou & Zhang, 2020; Ngou *et al.*, 2021; Pruitt *et al.*, 2021b;
332 Sun *et al.*, 2021; Tian *et al.*, 2021). Accordingly, a large number of DEGs in our assay were
333 annotated as disease resistance (R) protein-coding genes, of which the TNL class was
334 particularly enriched in BIR1 overexpressing plants (Swiderski *et al.*, 2009) **(Table S7)**.

335 Conversely, neither NON-RACE SPECIFIC DISEASE RESISTANCE 1 (NDR1) nor genes
336 encoding CNL intracellular receptors, which require NDR1, were differentially expressed in
337 response to BIR1 overexpression **(Fig. 4b) (Table S3)**.

338 EDS5, which transduces the signal downstream of SA in Arabidopsis (Nawrath *et al.*, 2002),
339 was up-regulated in DEX-treated BIR1 L9 samples. Interestingly, BIR2 was up-regulated,
340 whereas BIR3 and its partner CONSTITUTIVE SHADE AVOIDANCE 1 (CSA1), which also
341 interacts with BIR1, were unaffected by BIR1 overexpression **(Fig. S6)** (Schulze *et al.*, 2022).
342 Finally, transcripts encoding the plant heterotrimeric G proteins ARABIDOPSIS G PROTEIN
343 α-SUBUNIT1 (GPA1), ARABIDOPSIS G PROTEIN β-SUBUNIT 1 (AGB1),
344 ARABIDOPSIS G PROTEIN γ-SUBUNIT 2 (AGG2), and EXTRA-LARGE G PROTEIN 1
345 and 2 (XLG1/2) were more abundant in plants overexpressing BIR1 relative to controls after
346 12 days of DEX treatment (**Fig. S7b**). These proteins positively regulate stomatal defense and
347 PTI signaling, ROS production and BIK1 stability allowing optimal immune activation (Liang
348 *et al.*, 2016; Zhong *et al.*, 2019). Consistent with transcript levels, SOBIR1, PAD4-dependent
349 PR1 and EDS1 proteins were strongly up-regulated by BIR1 overexpression in DEX-treated
350 BIR1 L9 plants, compared to the non-treated controls (**Figs. 4c, 5c**).

351 In conclusion, in the absence of microbes or microbe-derived elicitors/effectors, the
352 expression of BIR1 at non-physiological levels alters hormone homeostasis, and leads to an
353 inadequate over-activation of multiple immune receptors and co-receptors involved in the
354 perception and signaling of ligands and effectors.

355

356 **Genetic disruption of SOBIR1, but not BAK1, partially rescues BIR1 overexpression**
357 **phenotypes**

358 In the following sections we tested if mutations in key components of PTI and ETI signaling
359 alleviated cell death and immune alterations caused by non-physiological expression of BIR1
360 (Rodriguez *et al.*, 2016; Freh *et al.*, 2022). SOBIR1 and BAK1 are necessary for activating cell
361 death and constitutive defense responses in the *bir1-1* mutant (Gao *et al.*, 2009; Liu *et al.*, 2016).
362 Therefore, we tested if SOBIR1 and BAK1 were also required for the BIR1 phenotypes. A
363 DEX-inducible BIR1-mCherry system was used to generate independent homozygous
364 transgenic lines in the well-characterized *sobir1-12* and *bak1-5* mutant backgrounds (Gao *et*
365 *al.*, 2009; Schwessinger *et al.*, 2011). Transgenic plants were sprayed with a 30 μM DEX

366 solution or H_2O (mock-treated controls) for 12 days at 24 h intervals to trigger BIR1
367 overexpression.

368 As previously shown, our reference set of DEX-treated BIR1 L9 plants accumulated high
369 levels of BIR1 transcripts, and displayed stunting symptoms, accelerated senescence, and cell
370 death relative to non-treated BIR1 L9 controls or DEX-treated WT plants **(Fig. 5a)** (Guzman-
371 Benito *et al.*, 2019). When *sobir1-12* BIR1 plants were investigated, we observed that the
372 phenotypes after 12 days of DEX treatments, albeit variable between biological replicates, were
373 milder than those in BIR1 L9 plants **(Figs. 5a, S8a,b)**. Interestingly, BIR1 transcript and protein
374 accumulated in *sobir1-12* BIR1 plants like in BIR1 L9 plants after 12 days of DEX application,
375 discarding potential dose effects **(Fig. 5b,c)**. Transcripts of the PTI-markers RBOHD, FRK1
376 and WRKY DNA-BINDING PROTEIN 29 (WRKY29), were increased, albeit not
377 significantly, in DEX-treated *sobir1-1*2 BIR1 plants relative to non-treated controls **(Figs. 5d,**
378 **S8c).** These finding suggest that cell death and PTI gene activation due to BIR1 overexpression
379 were alleviated by the lack of SOBIR1.

380 *bak1*-5 BIR1 plants consistently developed strong morphological phenotypes after 12 days
381 of DEX application, that closely resemble those of BIR1 L9 plants **(Figs. 5a, S8a,b)**. RT-qPCR
382 showed that BIR1 transcripts also accumulated in these plants after long DEX treatments,
383 although to a variable degree depending on the transgenic lines and biological replicates. For
384 instance, BIR1 transcript levels in *bak1*-5 BIR1 plants were comparable to those in *sobir1-12*
385 BIR1 plants in **Fig. S8b**. Differences in BIR1 protein accumulation were observed between
386 DEX-treated *bak1-5* BIR1 L4 and L10 lines in this experiment **(Fig. 5c)**. **Figs. 5a** and **b**
387 illustrate data from a different experimental replicate in which BIR1 transcripts in *bak1*-5 BIR1
388 plants were much less abundant than in BIR1 L9 plants. These interesting observations suggest
389 that the persistent induction of BIR1 over time, rather than an excess of BIR1, was the trigger
390 of the morphological alterations in the *bak1*-5 mutant background. RBOHD, FRK1 and WRKY
391 remained transcriptionally up-regulated in DEX-treated *bak1-5* BIR1 plants although at varying
392 degrees between replicates **(Fig. 5e)**. Collectively, these data indicate that the morphological
393 phenotypes and, perhaps, PTI gene activation when BIR1 is expressed at non-physiological
394 levels are genetically unrelated to BAK1.

395 Alterations in plant hormone pathways may negatively affect plant growth (Denance *et al.*,
396 2013). The transcriptional reprogramming of genes involved in plant hormone metabolism and
397 signaling in BIR1-overexpressing plants prompted us to further examine their expression in the
398 mutant backgrounds mentioned above. RT-qPCR revealed that genes encoding salicylic acid

399 (SA)-dependent PR1, jasmonic acid (JA)-responsive PLANT DEFENSIN 1.2 (PDF1.2),
400 ethylene (ET)- and JA-responsive PR4 as well as genes encoding the cytochrome P450 enzymes
401 CYP71B15 (PAD3) and CYP79B2 involved in camalexin (CA)-biosynthesis and CA-mediated
402 plant defense, were all up-regulated in BIR1-overexpressing plants of *sobir1-12* BIR1
403 genotypes **(Fig. 5f)**. Intriguingly, the induction of phytohormone-related genes was notably
404 reduced in *bak1-5* BIR1 plants after DEX treatment compared to *sobir1-12* BIR1 or BIR1 L9
405 plants **(Figs. 4a, 5g)**. This data suggests that the *bak1-5* mutation may, at least partially,
406 compromise hormone defense signaling upon BIR1 overexpression. None of these genes,
407 except PR1, were induced or repressed in DEX-treated WT plants, discarding a potential effect
408 of DEX on their expression **(Table S3)**.

409

410 **Genetic disruption of EDS1, but not PAD4, partially rescues BIR1 overexpression**
411 **phenotypes**

412 A previous report showed that stunting, activation of cell death and defense responses in the
413 *bir1-1* mutant were partially dependent on EDS1 and PAD4 (Gao *et al.*, 2009). The EDS1-
414 PAD4 node has a relevant role in PRR signaling and TNL activation, indicating that it mediates
415 both PTI and ETI (Pruitt *et al.*, 2021a). We had observed that TNL-coding transcripts were
416 abundant in BIR1 L9 plants and that EDS1 transcripts and protein were elevated in BIR1 L9,
417 *sobir1-12* BIR1 and *bak1-5* BIR1 plants (**Figs. 5b,c**). Therefore, we wondered if TNL-mediated
418 ETI responses along with, or independently of, PTI could be important for BIR1 overexpression
419 phenotypes. Thus, we tested if the BIR1 phenotypes were affected by EDS1 or PAD4
420 mutations. The DEX-inducible BIR1-mCherry system was used to generate homozygous
421 transgenic lines from *eds1-2* and *pad4-1* mutants (Parker *et al.*, 1996; Zhou *et al.*, 1998). The
422 *eds1-2* BIR1 plants displayed mostly WT-like morphologies and, occasionally, localized
423 yellowing after 12 days of DEX treatments compared to non-treated plants **(Figs. 6a, S8a)**. RT-
424 qPCR analysis showed that BIR1 accumulated in the *eds1-2* BIR1 plants as much as in the
425 BIR1 L9 plants **(Figs. 6a)**. The expression of FRK1 and RBOHD was significantly enhanced
426 in *eds1-2* BIR1 plants after DEX applications compared to non-treated controls **(Fig. 6b)**.
427 WRKY29 showed a tendency, albeit not significant, to be up-regulated in these plants (Fig. 6b).
428 Our data indicated that the lack of EDS1 attenuates the phenotypic alterations caused by BIR1
429 overexpression, but does not affect the activation of PTI genes.

430 Next, we found that *pad4-1* BIR1 plants essentially had BIR1 L9-like phenotypes after 12
431 days of DEX applications **(Figs. 6a, S8a)**. In these plants, BIR1 accumulated much less than in
432 BIR1 L9 or *eds1-2* BIR1 plants **(Fig. 6a)**. As shown previously for *bak1-5* BIR1 plants, the
433 sustained induction of BIR1, rather than BIR1 overexpression, might be sufficient to cause
434 typical BIR1 phenotypes regardless of the *pad4-1* mutation. Interestingly, the PTI-components
435 FRK1, WRKY29 and RBOHD showed no responsiveness to BIR1 overexpression in *pad4-1*
436 BIR1 plants, which suggests that PTI gene activation in these plants is PAD4-dependent **Figs.
437 6c, S8c)**. In summary, the genetic elimination of EDS1, but not PAD4, mitigates the
438 morphological phenotypes caused by the induction of BIR1 at non-physiological levels. Likely,
439 symptoms arise from the activation of EDS1-dependent ETI-type cell death in BIR1
440 overexpressing plants, which is independent of PTI gene activation.

441 RT-qPCR revealed a significant transcriptional activation of genes encoding markers in the
442 SA, JA, ET and CA pathways in DEX-treated *eds1-2* BIR1 plants versus non-treated controls
443 **(Fig. 6d)**. PDF1.2 and PR4 transcript markers were also up-regulated, but to a lesser extent, in
444 *pad4*-1 BIR1 transgenic plants after 12 days of DEX treatments relative to the non-treated
445 controls, whereas PAD4-dependent PR1 and PAD3 transcripts were not differentially
446 expressed, suggesting that PAD4 was important for PTI gene expression and phytohormone
447 homeostasis **(Fig. 6e)**.

448

449 **Phenotypes of BIR1 overexpressing lines are unrelated to SA signaling pathways**

450 *pad4-1* BIR1 plants were as sensitive to DEX treatments as BIR1 L9 plants, suggesting that
451 morphological phenotypes caused by non-physiological BIR1 levels are independent of SA-
452 mediated signaling. To confirm this prediction, the effects of mutations in SALICYLIC ACID
453 INDUCTION DEFICIENT 2 (SID2) and EDS5, involved in pathogen-induced SA biosynthesis
454 (Huang *et al.*, 2020), were assessed in BIR1 overexpressing plants. DEX-inducible BIR1-
455 mCherry transgenic plants were generated in the *sid2-2* and *eds5-3* (*eds5* is allelic to *sid1*)
456 backgrounds, which contain low levels of SA (Nawrath *et al.*, 2002). We found that *sid2-2*
457 BIR1 plants exhibited from moderate to severe morphological phenotypes after 12 days of DEX
458 treatment. These coincided with moderate levels of BIR1 overexpression relative to those
459 observed in BIR1 L9 plants **(Figs. 7a)**. The transcription levels of PR4, PDF1.2, PAD3 and
460 CYP79B2 were significantly elevated in DEX-treated *sid2*-2 BIR1 plants compared to non-
461 treated controls **(Fig. 7b)**. *eds5*-3 BIR1 plants typically displayed strong developmental defects

462 and necrosis and accumulated BIR1 transcripts at BIR1 L9-like levels after long DEX
463 applications **(Figs. 7a)**. PR4, PAD3 and PDF1.2, but not CYP79B2, were up-regulated in *eds5-*
464 *3* BIR1 overexpressing plants relative to non-treated controls **(Fig. 7c)**. Interestingly, the
465 canonical SA-marker PR1 was also induced in *eds5-3* BIR1 and, to a much lesser extent, *sid2-*
466 2 BIR1 plants. This observation suggests that PR1 induction was only partially dependent on
467 EDS5 and SID2 in these plants (Tsuda *et al.*, 2013) **(Fig. 7b,c)**. Although residual EDS5/SID2-
468 independent SA production in BIR1 overexpressing plants cannot be fully discarded (Lu, 2009),
469 our findings suggest that the ETI-like phenotypes in these plants were not drastically affected
470 by mutations in SA biosynthesis (*sid2-2* and *eds5-3*) and SA signaling (*pad4-1*). This idea is
471 consistent with the observation that the expression of most SA-responsive genes, including
472 PR1, is also controlled by SA-independent mechanisms during EDS1-dependent ETI (Tsuda *et*
473 *al.*, 2013; Cui *et al.*, 2017).

474

475 **Discussion**

476 Plants respond to microbes and viruses by enhancing the expression of multiple genes that
477 function as regulators or executors of defense programs (Nishad *et al.*, 2020). Among them,
478 BIR1 was shown to be up-regulated during bacterial and oomycete infections, and also during
479 viral infections in a SA-dependent manner (Gao *et al.*, 2009; Guzman-Benito *et al.*, 2019). The
480 observation that knock-out *bir1-1* mutants have increased resistance to the virulent oomycete
481 *Hyaloperonospora parasitica* Noco2 and to the RNA virus *Tobacco rattle virus* (TRV) suggests
482 an active role of BIR1 in plant immunity (Gao *et al.*, 2009; Guzman-Benito *et al.*, 2019). Since
483 BIR1 is a negative regulator of cell death and defense (Liu *et al.*, 2016), we hypothesized that
484 BIR1 induction might be part of a common strategy to modulate, at least partially, the amplitude
485 of the immune responses during microbial and viral infections. To test this hypothesis, we used
486 a previously described DEX-inducible system for the conditional expression of a mCherry-
487 tagged BIR1 transgene in Arabidopsis (Guzman-Benito *et al.*, 2019). By using different
488 induction times, this system allowed us to investigate the outputs associated with physiological
489 and non-physiological levels of BIR1. Even though adverse effects due to long DEX treatments
490 cannot be fully discarded in our experimental system, specific effects resulting from BIR1
491 overexpression could be distinguished from other potential combinatorial effects resulting from
492 expressing BIR1 in an activated glucocorticoid-inducible background (Kang *et al.*, 1999).
493 Importantly, BIR1 induction is triggered in the absence of immune elicitors or effectors that
494 could otherwise initiate undesirable localized and systemic defense responses in the plant.

495 The induction of BIR1 at a level comparable to that observed under natural conditions in
496 bacteria- or virus-infected plants, or plants treated with SA was referred to as physiological in
497 our assay (Gao *et al.*, 2009; Guzman-Benito *et al.*, 2019). At this level, BIR1 had a subtle, if
498 any, impact on both plant transcriptome and plant morphology. In contrast, in the presence of
499 the PTI elicitor flg22, the induction of BIR1 negatively affects the expression of several PTI-
500 marker genes, but has no effects on ROS burst, as previously shown (Liu *et al.*, 2016), or
501 ethylene production. This observation suggests that BIR1 can regulate, directly or indirectly,
502 the activity of components in the PTI signaling pathway that ultimately control immune gene
503 transcription. Furthermore, the physiological induction of BIR1 compromises the callose
504 deposition at PD elicited by either flg22 or the dsRNA-analog poly(I:C). Targeted deposition
505 of callose modulates symplastic connectivity by regulating PD pore size, and therefore
506 constitutes an essential layer in the defense against pathogens (Wang *et al.*, 2021). According
507 to our data, BIR1 induction during pathogen attacks can be interpreted as a strategy to regulate
508 PD trafficking. Although not tested in this study, BIR1 effects on gene expression and callose
509 deposition may render PTI less effective against pathogens. Indeed, PTI gene expression and
510 callose formation are usually blocked/inhibited by many defense-suppressing virulence
511 effectors from different types of microbes (Cui *et al.*, 2009; Wang *et al.*, 2021). Viral-encoded
512 proteins such as the potyviral silencing suppressor helper-component proteinase (HC-Pro) or
513 the movement protein (MP) of several tobamoviruses are capable of suppressing callose
514 deposition (Citovsky *et al.*, 1990; Chowdhury *et al.*, 2020). A recent work shows that
515 tobamovirus MPs promote viral cell-to-cell propagation by blocking dsRNA-induced callose
516 deposition (Huang *et al.*, 2023). It is tempting to speculate that BIR1 induction during the viral
517 infection controls PD callose deposition, and perhaps other antiviral defenses, triggered by
518 virus-derived dsRNA. Further research is needed to test these ideas.

519 The overexpression of BIR1 at a level as that expected when BIR1 gene regulation is lost
520 was referred to as non-physiological. At this level, BIR1 led to cell death-type morphological
521 phenotypes, and the inappropriate overexpression of plant immune genes (Guzman-Benito *et*
522 *al.*, 2019). Among them, the up-regulation of a significant number of RLP-coding genes is
523 striking. RLPs have been observed to be predominantly expressed in plants undergoing leaf
524 senescence, supporting the idea that BIR1 overexpression accelerates a senescence program
525 (Wang *et al.*, 2008). In Arabidopsis, RLP1, RLP23, RLP30, RLP32 and RLP42 mediate
526 SOBIR1-dependent immune activation, but the role of other RLPs in the perception of pathogen
527 and defense is unknown (Wang *et al.*, 2008; Zhang *et al.*, 2013; Albert *et al.*, 2019).

528 The overexpression of genes encoding TNL-resistance proteins, but not CNLs, is another
529 important feature linked to the non-physiological induction of BIR1. TNL-based immunity is
530 mediated by two distinct signaling modules, EDS1/SAG101/NRG1 and EDS1/PAD4/ADR1
531 (Sun *et al.*, 2021). Here, we provide genetic evidence that the BIR1 overexpression
532 morphological phenotypes are partially dependent on EDS1, but not on PAD4 . We propose
533 that EDS1, perhaps in concert with SAG101, triggers cell death-like phenotypes upon TNL
534 activation in BIR1 overexpressing plants **(Fig. 7d)**. How TNL receptors are activated when
535 BIR1 is strongly expressed is a question to resolve. A current model postulates that loss of BIR1
536 function leads to the activation of hypothetical guarding R proteins which further feed PAD4-
537 and SOBIR1-dependent resistance pathways (Gao *et al.*, 2009). Our results are coherent with
538 BIR1 or a yet unknown BIR1/SERK complex being guarded by one or several EDS1-dependent
539 TNL proteins. Therefore, induction of BIR1 at non-physiological leves may promote TNL-
540 mediated resistance pathways that require EDS1 when no effectors or elicitors are present.

541 In addition to EDS1, we demonstrated that SOBIR1 is necessary for BIR1 overexpression
542 phenotypes. The role of SOBIR1 in the BIR1 pathway is unclear. Although extensive
543 investigation is required, SOBIR1 may function as a specific co-regulator of the EDS1-
544 dependent responses triggered by BIR1 overexpression, as part of the same signaling pathway
545 **(Fig. 7d)**. This idea is inspired by a recent work showing that the cell-surface RLP23 receptor
546 uses SOBIR1 to form a supramolecular complex with a EDS1/PAD4/ADR1 node in a ligand-
547 independent manner to mediate defense signaling cascades that are common to both surface
548 PRR (PTI) and NLR (ETI) receptors (Pruitt *et al.*, 2021b).

549 The TNL protein CSA1 senses perturbances of BIR3, BAK1 or BIR3/BAK1 complexes
550 leading to ETI-type autoimmune responses (Schulze *et al.*, 2022). CSA1 did not show
551 responsiveness to BIR1 overexpression in our assay, but it has been shown to interact with
552 BIR1 (Schulze *et al.*, 2022). It will be interesting to see if CSA1 also guards BIR1 integrity,
553 perhaps in cooperation with SOBIR1 and/or other SERKs **(Fig. 7d)**. Finally, phenotypes linked
554 to BIR1 overexpression were apparently unaffected by the *bak1-5* mutation, which suggests
555 that other SERK family members can compensate for the loss of BAK1 in PTI/ETI signaling.

556 We observed that the upregulation of FRK1, WRKY29 and RBOHD due to BIR1
557 overexpression was compromised by mutations in SOBIR1 and PAD4, but it was independent
558 of EDS1. Since EDS1, PAD4 and SOBIR1 are important for both cell surface PRR receptor-
559 and TNL-mediated signaling and resistance (Pruitt *et al.*, 2021b; Tian *et al.*, 2021), we will
560 need additional experimentation to establish if changes in PTI gene expression involve PTI-

561 dependent pathways, TNL activation or other unknown mechanisms yet to be determined. Our
562 study also reveals significant alterations in plant hormone gene expression caused by non-
563 physiological levels of BIR1. Interestingly, genes related to the plant hormones ET, JA, CA,
564 and SA, which play a central role in regulating immune responses, remained up-regulated in
565 *eds1-2* BIR1 and *sobir1-12* BIR1 backgrounds, in which phenotypes were partially rescued.
566 This suggests that i) regulation of hormone homeostasis does not require SOBIR1- and/or
567 EDS1-mediated signaling pathways, and that ii) such hormonal imbalance in BIR1
568 overexpressing plants has little, if any, influence on the ETI-like phenotypes.

569 The Arabidopsis heterotrimeric G protein AGB1 (SOBIR2) is a common signaling
570 component of PTI mediated by different RLK-PRRs, and functions in parallel with PAD4
571 downstream of SOBIR1 to regulate cell death and pathogen resistance in *bir1-1* Arabidopsis
572 mutants (Liu *et al.*, 2013; Liang *et al.*, 2016). Similarly, Gγ-proteins AGG1/AGG2 have been
573 described as positive regulators of cell death and constitutive defense phenotypes in *bir1-1*
574 mutants (Liu *et al.*, 2013). AGB1 and AGG2 were up-regulated in BIR1 overexpressing plants.
575 These findings bring up the idea that AGB1 and AGG1/2 could also function downstream of
576 BIR1 to regulate EDS1-mediated cell death when BIR1 integrity is disrupted. Equally
577 important, the BIR1-responsive GPA1 and XLG, in association with Gβγ modules, also have
578 crucial roles in multiple growth and developmental processes (Wang *et al.*, 2023). Thus, it is
579 conceivable that overactivation of these heterotrimeric G proteins due to expression of BIR1 at
580 non-physiological levels may cause indirect effects on plant development. Further studies are
581 needed to test these plausible hypotheses and their applicability to other plants species. In
582 addition, identification of BIR1 interactors shall increase our understanding of the underlying
583 mechanisms and components of the BIR1-mediated regulation of immunity.

584

585 **Conclusions**

586 Here, we investigated the implications of BIR1 homeostasis on the immune response in
587 Arabidopsis. BIR1 induction at physiological levels interferes with both immune gene
588 expression and PD callose deposition triggered by canonical PTI elicitors. We posit that BIR1
589 induction may be a pathogen-driven mechanism to modulate plant defenses during infections,
590 helping to maintain a host-pathogen equilibrium. Expression of BIR1 at non-physiological
591 levels results in severe morphological and growth defects as well as transcriptomic changes
592 related to plant immunity, which suggests a dose-dependent regulatory activity of BIR1. We

593 show that both EDS1 and SOBIR1 are necessary for the ETI-type cell death phenotypes
594 observed when BIR1 is overexpressed, while PAD4 and BAK1 are not. We hypothesize that
595 BIR1, previously thought to represent a negative regulator of plant immunity, is a guarded
596 protein surveilled by unknown TNLs, with SOBIR1 working alongside EDS1 to transduce
597 signals downstream of the TNLs **(Fig. 7d)**.

598

599 **Acknowledgements**

600 This work was supported by National Research grants RTI2018-096979-B-I00 and PID2021
601 127982NB-I00 to CL from Ministerio de Ciencia e Innovación (Spain) and UE-FEDER, and
602 grant iLINKA20415 to CL from CSIC (Spain). Contributions of ARS, LEG and MH were
603 supported by grants ERA-NET SusCrop2 / ANR-21-SUSC-0003-01 and ANR-PRC / ANR-21-
604 CE20-0020-01 to MH. Contributions of CH and TN were supported by DFG grant Nu70/17-1
605 to TN.

606

607 **Author contributions**

608 CL and IGB conceived and designed the study. CL, IGB, CR and IP performed expression
609 assays and transgenics. CL and CH performed ROS and ethylene assays. CL, ARS and LEG
610 performed callose assays. CL, IGB, MH and TN analyzed the data. CL wrote the article.

611

612 **Competing interests**

613 None declared

614

615 **REFERENCES**

616 **Albert I, Zhang L, Bemm H, Nurnberger T. 2019.** Structure-Function Analysis of Immune
617 Receptor AtRLP23 with Its Ligand nlp20 and Coreceptors AtSOBIR1 and AtBAK1. *Mol*
618 *Plant Microbe Interact* **32**(8): 1038-1046.

619 **Belkhadir Y, Jaillais Y, Epple P, Balsemao-Pires E, Dangl JL, Chory J. 2012.**
620 Brassinosteroids modulate the efficiency of plant immune responses to microbe-associated
621 molecular patterns. *Proc Natl Acad Sci U S A* **109**(1): 297-302.

622 **Bi G, Zhou Z, Wang W, Li L, Rao S, Wu Y, Zhang X, Menke FLH, Chen S, Zhou JM.**
623 **2018.** Receptor-Like Cytoplasmic Kinases Directly Link Diverse Pattern Recognition
624 Receptors to the Activation of Mitogen-Activated Protein Kinase Cascades in Arabidopsis.
625 *Plant Cell* **30**(7): 1543-1561.
626 **Boudsocq M, Willmann MR, McCormack M, Lee H, Shan L, He P, Bush J, Cheng SH,**
627 **Sheen J. 2010.** Differential innate immune signalling via Ca(2+) sensor protein kinases.
628 *Nature* **464**(7287): 418-422.
629 **Boutrot F, Zipfel C. 2017.** Function, Discovery, and Exploitation of Plant Pattern Recognition
630 Receptors for Broad-Spectrum Disease Resistance. *Annu Rev Phytopathol* **55**: 257-286.
631 **Castro B, Citterico M, Kimura S, Stevens DM, Wrzaczek M, Coaker G. 2021.** Stress-
632 induced reactive oxygen species compartmentalization, perception and signalling. *Nat*
633 *Plants* **7**(4): 403-412.
634 **Chen Z. 2001.** A superfamily of proteins with novel cysteine-rich repeats. *Plant Physiol* **126**(2):
635 473-476.
636 **Chowdhury RN, Lasky D, Karki H, Zhang Z, Goyer A, Halterman D, Rakotondrafara**
637 **AM. 2020.** HCPro Suppression of Callose Deposition Contributes to Strain-Specific
638 Resistance Against Potato Virus Y. *Phytopathology* **110**(1): 164-173.
639 **Citovsky V, Knorr D, Schuster G, Zambryski P. 1990.** The P30 movement protein of tobacco
640 mosaic virus is a single-strand nucleic acid binding protein. *Cell* **60**(4): 637-647.
641 **Clough SJ, Bent AF. 1998.** Floral dip: a simplified method for Agrobacterium-mediated
642 transformation of Arabidopsis thaliana. *Plant J* **16**(6): 735-743.
643 **Couto D, Zipfel C. 2016.** Regulation of pattern recognition receptor signalling in plants. *Nat*
644 *Rev Immunol* **16**(9): 537-552.
645 **Cui H, Gobbato E, Kracher B, Qiu J, Bautor J, Parker JE. 2017.** A core function of EDS1
646 with PAD4 is to protect the salicylic acid defense sector in Arabidopsis immunity. *New*
647 *Phytol* **213**(4): 1802-1817.
648 **Cui H, Xiang T, Zhou JM. 2009.** Plant immunity: a lesson from pathogenic bacterial effector
649 proteins. *Cell Microbiol* **11**(10): 1453-1461.
650 **Denance N, Sanchez-Vallet A, Goffner D, Molina A. 2013.** Disease resistance or growth: the
651 role of plant hormones in balancing immune responses and fitness costs. *Front Plant Sci* **4**:
652 155.
653 **Dominguez-Ferreras A, Kiss-Papp M, Jehle AK, Felix G, Chinchilla D. 2015.** An Overdose
654 of the Arabidopsis Coreceptor BRASSINOSTEROID INSENSITIVE1-ASSOCIATED

655 RECEPTOR KINASE1 or Its Ectodomain Causes Autoimmunity in a SUPPRESSOR OF
656 BIR1-1-Dependent Manner. *Plant Physiol* **168**(3): 1106-1121.
657 **Freh M, Gao JL, Petersen M, Panstruga R. 2022.** Plant autoimmunity-fresh insights into an
658 old phenomenon. *Plant Physiology* **188**(3): 1419-1434.
659 **Gao M, Wang X, Wang D, Xu F, Ding X, Zhang Z, Bi D, Cheng YT, Chen S, Li X, et al.**
660 **2009.** Regulation of cell death and innate immunity by two receptor-like kinases in
661 Arabidopsis. *Cell Host Microbe* **6**(1): 34-44.
662 **Gust AA, Pruitt R, Nurnberger T. 2017.** Sensing Danger: Key to Activating Plant Immunity.
663 *Trends Plant Sci* **22**(9): 779-791.
664 **Guzman-Benito I, Donaire L, Amorim-Silva V, Vallarino JG, Esteban A, Wierzbicki AT,**
665 **Ruiz-Ferrer V, Llave C. 2019.** The immune repressor BIR1 contributes to antiviral defense
666 and undergoes transcriptional and post-transcriptional regulation during viral infections.
667 *New Phytol* **224**(1): 421-438.
668 **Halter T, Imkampe J, Mazzotta S, Wierzba M, Postel S, Bucherl C, Kiefer C, Stahl M,**
669 **Chinchilla D, Wang X, et al. 2014.** The leucine-rich repeat receptor kinase BIR2 is a
670 negative regulator of BAK1 in plant immunity. *Curr Biol* **24**(2): 134-143.
671 **Hohmann U, Lau K, Hothorn M. 2017.** The Structural Basis of Ligand Perception and Signal
672 Activation by Receptor Kinases. *Annu Rev Plant Biol* **68**: 109-137.
673 **Huang C, Sede AR, Elvira-González L, Yan Y, Rodriguez M, Mutterer J, Boutant E, Shan**
674 **L, Heinlein M. 2023.** dsRNA-induced immunity targets plasmodesmata and is suppressed
675 by viral movement proteins. *Plant Cell* **35**(10): 3845-3869.
676 **Huang W, Wang Y, Li X, Zhang Y. 2020.** Biosynthesis and Regulation of Salicylic Acid and
677 N-Hydroxypipecolic Acid in Plant Immunity. *Mol Plant* **13**(1): 31-41.
678 **Imkampe J, Halter T, Huang S, Schulze S, Mazzotta S, Schmidt N, Manstretta R, Postel**
679 **S, Wierzba M, Yang Y, et al. 2017.** The Arabidopsis Leucine-Rich Repeat Receptor Kinase
680 BIR3 Negatively Regulates BAK1 Receptor Complex Formation and Stabilizes BAK1.
681 *Plant Cell* **29**(9): 2285-2303.
682 **Jubic LM, Saile S, Furzer OJ, El Kasmi F, Dangl JL. 2019.** Help wanted: helper NLRs and
683 plant immune responses. *Curr Opin Plant Biol* **50**: 82-94.
684 **Kadota Y, Sklenar J, Derbyshire P, Stransfeld L, Asai S, Ntoukakis V, Jones JD, Shirasu**
685 **K, Menke F, Jones A, et al. 2014.** Direct regulation of the NADPH oxidase RBOHD by the
686 PRR-associated kinase BIK1 during plant immunity. *Mol Cell* **54**(1): 43-55.
687 **Kang HG, Fang YW, Singh KB. 1999.** A glucocorticoid-inducible transcription system causes
688 severe growth defects in

689 and induces defense-related genes. *Plant Journal* **20**(1): 127-133.
690 **Korner CJ, Klauser D, Niehl A, Dominguez-Ferreras A, Chinchilla D, Boller T, Heinlein**
691 **M, Hann DR. 2013.** The immunity regulator BAK1 contributes to resistance against diverse
692 RNA viruses. *Mol Plant Microbe Interact* **26**(11): 1271-1280.
693 **Li L, Li M, Yu L, Zhou Z, Liang X, Liu Z, Cai G, Gao L, Zhang X, Wang Y, et al. 2014.**
694 The FLS2-associated kinase BIK1 directly phosphorylates the NADPH oxidase RbohD to
695 control plant immunity. *Cell Host Microbe* **15**(3): 329-338.
696 **Li P, Lu YJ, Chen H, Day B. 2020.** The Lifecycle of the Plant Immune System. *CRC Crit Rev*
697 *Plant Sci* **39**(1): 72-100.
698 **Liang X, Ding P, Lian K, Wang J, Ma M, Li L, Li L, Li M, Zhang X, Chen S, et al. 2016.**
699 Arabidopsis heterotrimeric G proteins regulate immunity by directly coupling to the FLS2
700 receptor. *Elife* **5**: e13568.
701 **Liang X, Zhou JM. 2018.** Receptor-Like Cytoplasmic Kinases: Central Players in Plant
702 Receptor Kinase-Mediated Signaling. *Annu Rev Plant Biol* **69**: 267-299.
703 **Liu J, Ding P, Sun T, Nitta Y, Dong O, Huang X, Yang W, Li X, Botella JR, Zhang Y.**
704 **2013.** Heterotrimeric G proteins serve as a converging point in plant defense signaling
705 activated by multiple receptor-like kinases. *Plant Physiol* **161**(4): 2146-2158.
706 **Liu Y, Huang X, Li M, He P, Zhang Y. 2016.** Loss-of-function of Arabidopsis receptor-like
707 kinase BIR1 activates cell death and defense responses mediated by BAK1 and SOBIR1.
708 *New Phytol* **212**(3): 637-645.
709 **Lu H. 2009.** Dissection of salicylic acid-mediated defense signaling networks. *Plant Signal*
710 *Behav* **4**(8): 713-717.
711 **Luna E, Pastor V, Robert J, Flors V, Mauch-Mani B, Ton J. 2011.** Callose deposition: a
712 multifaceted plant defense response. *Mol Plant Microbe Interact* **24**(2): 183-193.
713 **Lv Y, Yang N, Wu J, Liu Z, Pan L, Lv S, Wang G. 2016.** New insights into receptor-like
714 protein functions in Arabidopsis. *Plant Signal Behav* **11**(7): e1197469.
715 **Mithoe SC, Menke FL. 2018.** Regulation of pattern recognition receptor signalling by
716 phosphorylation and ubiquitination. *Curr Opin Plant Biol* **45**(Pt A): 162-170.
717 **Nawrath C, Heck S, Parinthawong N, Metraux JP. 2002.** EDS5, an essential component of
718 salicylic acid-dependent signaling for disease resistance in Arabidopsis, is a member of the
719 MATE transporter family. *Plant Cell* **14**(1): 275-286.
720 **Ngou BPM, Ahn HK, Ding P, Jones JDG. 2021.** Mutual potentiation of plant immunity by
721 cell-surface and intracellular receptors. *Nature* **592**(7852): 110-115.

722 **Nishad R, Ahmed T, Rahman VJ, Kareem A. 2020.** Modulation of Plant Defense System in
723 Response to Microbial Interactions. *Front Microbiol* **11**: 1298.
724 **Parker JE, Holub EB, Frost LN, Falk A, Gunn ND, Daniels MJ. 1996.** Characterization of
725 eds1, a mutation in Arabidopsis suppressing resistance to Peronospora parasitica specified
726 by several different RPP genes. *Plant Cell* **8**(11): 2033-2046.
727 **Pruitt RN, Gust AA, Nurnberger T. 2021a.** Plant immunity unified. *Nat Plants* **7**(4): 382-
728 383.
729 **Pruitt RN, Locci F, Wanke F, Zhang L, Saile SC, Joe A, Karelina D, Hua C, Frohlich K,**
730 **Wan WL, et al. 2021b.** The EDS1-PAD4-ADR1 node mediates Arabidopsis pattern-
731 triggered immunity. *Nature* **598**(7881): 495-499.
732 **Quezada EH, Garcia GX, Arthikala MK, Melappa G, Lara M, Nanjareddy K. 2019.**
733 Cysteine-Rich Receptor-Like Kinase Gene Family Identification in the Phaseolus Genome
734 and Comparative Analysis of Their Expression Profiles Specific to Mycorrhizal and
735 Rhizobial Symbiosis. *Genes (Basel)* **10**(1).
736 **Rao S, Zhou Z, Miao P, Bi G, Hu M, Wu Y, Feng F, Zhang X, Zhou JM. 2018.** Roles of
737 Receptor-Like Cytoplasmic Kinase VII Members in Pattern-Triggered Immune Signaling.
738 *Plant Physiol* **177**(4): 1679-1690.
739 **Rodriguez E, El Ghoul H, Mundy J, Petersen M. 2016.** Making sense of plant autoimmunity
740 and 'negative regulators'. *FEBS J* **283**(8): 1385-1391.
741 **Schulze S, Yu L, Hua C, Zhang L, Kolb D, Weber H, Ehinger A, Saile SC, Stahl M, Franz-**
742 **Wachtel M, et al. 2022.** The Arabidopsis TIR-NBS-LRR protein CSA1 guards BAK1-BIR3
743 homeostasis and mediates convergence of pattern- and effector-induced immune responses.
744 *Cell Host Microbe* **30**(12): 1717-1731 e1716.
745 **Schwessinger B, Roux M, Kadota Y, Ntoukakis V, Sklenar J, Jones A, Zipfel C. 2011.**
746 Phosphorylation-dependent differential regulation of plant growth, cell death, and innate
747 immunity by the regulatory receptor-like kinase BAK1. *PLoS Genet* **7**(4): e1002046.
748 **Smakowska-Luzan E, Mott GA, Parys K, Stegmann M, Howton TC, Layeghifard M,**
749 **Neuhold J, Lehner A, Kong J, Grunwald K, et al. 2018.** An extracellular network of
750 Arabidopsis leucine-rich repeat receptor kinases. *Nature* **553**(7688): 342-346.
751 **Sun X, Lapin D, Feehan JM, Stolze SC, Kramer K, Dongus JA, Rzemieniewski J,**
752 **Blanvillain-Baufume S, Harzen A, Bautor J, et al. 2021.** Pathogen effector recognition-
753 dependent association of NRG1 with EDS1 and SAG101 in TNL receptor immunity. *Nat*
754 *Commun* **12**(1): 3335.

755 **Swiderski MR, Birker D, Jones JD. 2009.** The TIR domain of TIR-NB-LRR resistance
756 proteins is a signaling domain involved in cell death induction. *Mol Plant Microbe Interact*
757 **22**(2): 157-165.
758 **Tang D, Wang G, Zhou JM. 2017.** Receptor Kinases in Plant-Pathogen Interactions: More
759 Than Pattern Recognition. *Plant Cell* **29**(4): 618-637.
760 **Tian H, Wu Z, Chen S, Ao K, Huang W, Yaghmaiean H, Sun T, Xu F, Zhang Y, Wang S,**
761 **et al. 2021.** Activation of TIR signalling boosts pattern-triggered immunity. *Nature*
762 **598**(7881): 500-503.
763 **Tsuda K, Mine A, Bethke G, Igarashi D, Botanga CJ, Tsuda Y, Glazebrook J, Sato M,**
764 **Katagiri F. 2013.** Dual regulation of gene expression mediated by extended MAPK
765 activation and salicylic acid contributes to robust innate immunity in Arabidopsis thaliana.
766 *PLoS Genet* **9**(12): e1004015.
767 **van Wersch S, Tian L, Hoy R, Li X. 2020.** Plant NLRs: The Whistleblowers of Plant
768 Immunity. *Plant Commun* **1**(1): 100016.
769 **Wan WL, Zhang L, Pruitt R, Zaidem M, Brugman R, Ma X, Krol E, Perraki A, Kilian J,**
770 **Grossmann G, et al. 2019.** Comparing Arabidopsis receptor kinase and receptor protein-
771 mediated immune signaling reveals BIK1-dependent differences. *New Phytol* **221**(4): 2080-
772 2095.
773 **Wang G, Ellendorff U, Kemp B, Mansfield JW, Forsyth A, Mitchell K, Bastas K, Liu CM,**
774 **Woods-Tor A, Zipfel C, et al. 2008.** A genome-wide functional investigation into the roles
775 of receptor-like proteins in Arabidopsis. *Plant Physiol* **147**(2): 503-517.
776 **Wang J, Chai J. 2020.** Structural Insights into the Plant Immune Receptors PRRs and NLRs.
777 *Plant Physiol* **182**(4): 1566-1581.
778 **Wang Y, Li X, Fan B, Zhu C, Chen Z. 2021.** Regulation and Function of Defense-Related
779 Callose Deposition in Plants. *Int J Mol Sci* **22**(5).
780 **Wang Y, Zhang H, Wang P, Zhong H, Liu W, Zhang S, Xiong L, Wu Y, Xia Y. 2023.**
781 Arabidopsis EXTRA-LARGE G PROTEIN 1 (XLG1) functions together with XLG2 and
782 XLG3 in PAMP-triggered MAPK activation and immunity. *J Integr Plant Biol* **65**(3): 825-
783 837.
784 **Withers J, Dong X. 2017.** Post-translational regulation of plant immunity. *Curr Opin Plant*
785 *Biol* **38**: 124-132.
786 **Wu Y, Gao Y, Zhan Y, Kui H, Liu H, Yan L, Kemmerling B, Zhou JM, He K, Li J. 2020.**
787 Loss of the common immune coreceptor BAK1 leads to NLR-dependent cell death. *Proc*
788 *Natl Acad Sci U S A* **117**(43): 27044-27053.

789 **Yeh YH, Chang YH, Huang PY, Huang JB, Zimmerli L. 2015.** Enhanced Arabidopsis
790 pattern-triggered immunity by overexpression of cysteine-rich receptor-like kinases. *Front*
791 *Plant Sci* **6**: 322.
792 **Yip Delormel T, Boudsocq M. 2019.** Properties and functions of calcium-dependent protein
793 kinases and their relatives in Arabidopsis thaliana. *New Phytol* **224**(2): 585-604.
794 **Yu TY, Sun MK, Liang LK. 2021.** Receptors in the Induction of the Plant Innate Immunity.
795 *Mol Plant Microbe Interact* **34**(6): 587-601.
796 **Yuan M, Cai B, Xin XF. 2023.** Plant immune receptor pathways as a united front against
797 pathogens. *PLoS Pathog* **19**(2): e1011106.
798 **Yuan M, Jiang Z, Bi G, Nomura K, Liu M, Wang Y, Cai B, Zhou JM, He SY, Xin XF.**
799 **2021a.** Pattern-recognition receptors are required for NLR-mediated plant immunity. *Nature*
800 **592**(7852): 105-109.
801 **Yuan M, Ngou BPM, Ding P, Xin XF. 2021b.** PTI-ETI crosstalk: an integrative view of plant
802 immunity. *Curr Opin Plant Biol* **62**: 102030.
803 **Zhang W, Fraiture M, Kolb D, Loffelhardt B, Desaki Y, Boutrot FF, Tor M, Zipfel C,**
804 **Gust AA, Brunner F. 2013.** Arabidopsis receptor-like protein30 and receptor-like kinase
805 suppressor of BIR1-1/EVERSHED mediate innate immunity to necrotrophic fungi. *Plant*
806 *Cell* **25**(10): 4227-4241.
807 **Zhong CL, Zhang C, Liu JZ. 2019.** Heterotrimeric G protein signaling in plant immunity. *J*
808 *Exp Bot* **70**(4): 1109-1118.
809 **Zhou JM, Zhang Y. 2020.** Plant Immunity: Danger Perception and Signaling. *Cell* **181**(5):
810 978-989.
811 **Zhou N, Tootle TL, Tsui F, Klessig DF, Glazebrook J. 1998.** PAD4 functions upstream from
812 salicylic acid to control defense responses in Arabidopsis. *Plant Cell* **10**(6): 1021-1030.

813

814 **Figure legends**

815 **Fig. 1.** Transcriptional reprogramming associated with BAK1-INTERACTING RECEPTOR-
816 LIKE KINASE 1 (BIR1) induction in Arabidopsis. (a) Morphology of representative BIR1
817 transgenic Arabidopsis plants (line 9, L9) under the control of a dexamethasone (DEX)-
818 inducible 35S promoter used for RNA-Seq experiments. Samples were collected after 4 or 12
819 days of 30 μM DEX treatment. H_2O-treated plants were used as controls. Relative expression
820 of the BIR1-coding gene based on the number of Fragments Per Kilobase of transcript sequence
821 per Millions of base-pairs sequenced (FPKM) (top) and Western blot using anti-mCherry
822 antibody (bottom) in samples used for RNA-Seq. Significant differences between DEX- and
823 mock-treated samples were analyzed using two-way ANOVA followed by Sidak´s multiple
824 comparison test; ***, adjusted *p*-value < 0.001. (b) Principal component analysis (PCA) of
825 RNA-Seq data. The PCA was performed using normalized RNA-Seq data of differentially
826 expressed genes (DEGs) between BIR1 L9 and wild-type (WT) plants after 4 and 12 days of
827 DEX treatment (DeL9_vs DeWT_). Each biological replicate is represented in the score plot.
828 The variance explained by each component (%) is given in parentheses. The sample
829 (DeL9_12b) with differential expression within the DEX-treated L9 group is indicated with
830 black arrows in (a) and (b). (c) Number of up-or down-regulated transcripts, with a $|\log_2$ (Fold-
831 Change)$| \geq 1$ and adjusted *p*-value ≤ 0.01, in each pairwise comparison is indicated. (d)
832 Scatterplot of selected gene ontology (GO) terms of DEGs. GO terms between WT and BIR1
833 L9 plants at 4 and 12 days after DEX-treatment (DeL9_ vs DeWT_) are shown. Dot size
834 represents the count of different genes and the color indicates significance of the term
835 enrichment. GO terms with adjusted *p*-value < 0.05 are significantly enriched. The kinase term
836 (indicated by an arrow) was exclusively assigned to BIR1 L9 plants. WT, wild-type Col-0; L9,
837 BIR1 L9 transgenic plants; De, DEX-treated plants; Mo, Mock-treated plants; _4, 4 days of
838 treatment; _12, 12 days of treatment.

839

840 **Fig. 2.** Effect of BAK1-INTERACTING RECEPTOR-LIKE KINASE 1 (BIR1) induction on
841 immune responses triggered by flg22 and nlp20 treatments. (a) Over time production of reactive
842 oxygen species (ROS) in dexamethasone (DEX)-treated wild-type (WT) and BIR1 L6 and L9
843 transgenic plants after elicitation of Arabidopsis leaf disks with 1 μM flg22 (left), 1 μM nlp20
844 (middle) or H_2O (right). Bars represent means ± SD of relative fluorescence units. (b) Ethylene
845 accumulation in BIR1 L6 and L9 transgenic plants after treatment with H_2O (mock), flg22 and
846 nlp20 at 1 μM or 100 nM concentration as indicated. Bars represent average values ± SD.

847 Within each elicitor/mock treatment, differences between DEX-treated (DEX+) and controls
848 (DEX-) were analyzed by two-way ANOVA followed by Sidak´s multiple comparison test. (c)
849 RT-qPCR analysis of the genes encoding the PTI-markers FLG22-INDUCED RECEPTOR-
850 LIKE KINASE 1 (FRK1) and PATHOGENESIS RELATED 1 (PR1) at 45 min after treatment
851 with H_2O (mock) or 1 µM flg22, and determined in DEX-treated (DEX+) versus non-treated
852 (DEX-) samples. (d) Immunoprecipitation of mCherry-BIR1 fusion proteins, indicated with an
853 arrowhead, from samples of BIR1 L6 and L9 plants used in (a) and (b) (left), and RT-qPCR
854 analysis of BIR1-coding transcripts in DEX-treated (DEX+) samples of BIR1 L6 and L9 plants
855 used in (c) (right). In all cases, RT-qPCR values from biologically independent samples were
856 normalized to the CBP20 internal control, and related to H_2O (mock)-treated plants, set to a
857 value of 1. Data are means ± SD analyzed by Kruskal-Wallis test; *, adjusted *p*-value <0.05.
858 Experiments were repeated three times with similar results.

859

860 **Fig. 3.** BAK1-INTERACTING RECEPTOR-LIKE KINASE 1 (BIR1) induction inhibits flg22-
861 and poly(I:C)-triggered callose accumulation at plasmodesmata (PD). Callose spots at PD were
862 visualized upon aniline blue staining of epidermal cells in response to bacterial flg22 (a) or
863 poly(I:C) (b) in BIR1 L9 transgenic Arabidopsis plants. Plants were previously sprayed with
864 30 µM dexamethasone (DEX) for three days to elicit BIR1 expression. Mock-treated plants
865 were used as non BIR1-expressing controls (top panels). Photographs were taken 30 minutes
866 after treatment with H_2O (control) or 1 µM flg22 or 50 ng/µl of poly(I:C). BIR1-mCherry
867 fluorescence in DEX-treated BIR1 L9 plants was confirmed within the same images. Inlays
868 show enlargements of the areas within the dashed boxes. Scale bar, 10 µm. (c) Relative PD
869 callose content in flg22/poly(I:C)-treated and H_2O (control)-treated leaves from BIR1 L9 plants
870 previously treated with or without DEX as indicated. d) Callose content at PD in control (DEX
871 -) and DEX-treated wild-type (WT) plants in response to H_2O and poly (I:C) is shown. In all
872 cases, black dots represent the mean values of callose intensities in individual PD (>100)
873 measured in three leaf discs taken from at least three independent biological replicates per each
874 treatment. Significant differences between samples were analyzed by Kruskal-Wallis test or by
875 one-way ANOVA followed by Tukey's multiple comparison test; ****, adjusted *p*-value
876 <0.0001, ***, <0.001, **, <0.01. Experiments were repeated twice with similar results.

877

878 **Fig. 4.** BAK1-INTERACTING RECEPTOR-LIKE KINASE 1 (BIR1) overexpression leads to
879 the transcriptional activation of pattern-triggered immunity (PTI)-associated co-receptors and
880 effector-triggered immunity (ETI) regulators. (a) Validation of the RNA-Seq results.
881 Expression of markers encoded by selected BIR1-responsive differentially expressed genes
882 (DEGs) after 12 days of dexamethasone (DEX) treatment based on fold-change values (log_2
883 DeL9_12/DeWT_12 and log_2 DeL9_12/MoL9_12 as indicated) was confirmed by RT-qPCR.
884 Values from biologically independent samples were normalized to the CBP20 internal control,
885 and related to untreated (DEX-) plants, set to a value of 1. Data are mean ± SD analyzed by
886 Mann-Whitney test; *, p <0.05. (b) Relative expression of selected genes encoding PTI/ETI-
887 markers based on the number of Fragments Per Kilobase of transcript sequence per Millions of
888 base-pairs sequenced (FPKM) in each of the three independent samples per condition used for
889 RNA-Seq. Actin expression is shown as control. Note that the expression levels of each
890 individual replicate within the DEX-treated BIR1 L9_12 group mirror the abundance of BIR1
891 transcripts in each replicate. DeL9_12b is indicated by a red arrow. Significant differences
892 between mock-treated and DEX-treated samples were analyzed using two-way ANOVA
893 followed by Sidak´s multiple comparison test; ****, adjusted p-value < 0.0001, *** < 0.001,
894 **< 0.01. WT, wild-type Col-0; L9, BIR1 L9 transgenics; _4d, 4 days of treatment; _12d, 12
895 days of treatment. (c) Western blot analysis of SUPPRESSOR OF BIR1-1 (SOBIR1) and
896 PATHOGENESIS RELATED 1 (PR1) using specific antibodies in two independent sets of
897 BIR1 L9 samples. Plants were mock-treated (-) or DEX-treated (+) for 12 days. The presence
898 (+) or absence (-) of morphological phenotypes (Ph) in each sample is indicated. Protein loading
899 control by Ponceau S is shown.

900

901 **Fig. 5.** Phenotypes caused by BAK1-INTERACTING RECEPTOR-LIKE KINASE 1 (BIR1)
902 overexpression are partially rescued in *sobir1-12* mutants, but not in a *bak1-5* mutant.
903 Morphology of transgenic *sobir1-12* BIR1 L6 and *bak1*-5 BIR1 L10 mutant plants expressing
904 BIR1 under the control of a dexamethasone (DEX)-inducible 35S promoter. Transgenic BIR1
905 L9 plants in the wild-type (WT) Col-0 background are shown as a reference. Plants were grown
906 for three weeks on soil and treated with 30 µM dexamethasone (DEX) to induce BIR1
907 transcription or mock-treated with H_2O. Non-transgenic WT Col-0 plants are shown as controls.
908 Plants were photographed after 12 days of the first DEX/ H_2O application. Images from
909 independent transgenic lines are shown in Fig. S7. RT-qPCR analysis of *BIR1* transcripts in
910 BIR1 L9 plants are shown. b) RT-qPCR analysis of BIR1 and ENHANCED DISEASE

911 SUSCEPTIBILITY 1 (EDS1) transcripts in *sobir1-12* BIR1 L6 and *bak1*-5 BIR1 L10 plants.
912 c) Western blot analysis of BIR1 and EDS1 proteins with specific antibodies in WT BIR1 L9
913 and two independent lines of *sobir1-12* BIR1 (L6, L8) and *bak1*-5 BIR1 (L4, L10). Plants were
914 mock-treated (-) or DEX-treated (+) for 12 days as indicated. The presence (+) or absence (-)
915 of morphological phenotypes (Ph) in each sample is indicated. Protein loading control by
916 Ponceau S is shown. RT-qPCR analysis of genes encoding the PTI-markers RESPIRATORY
917 BURST OXIDASE HOMOLOG PROTEIN D (RBOHD), FLG22-INDUCED RECEPTOR-
918 LIKE KINASE 1 (FRK1) or WRKY DNA-BINDING PROTEIN 29 (WRKY29) in *sobir1-12*
919 BIR1 L6 (d) and *bak1*-5 BIR1 L10 (e) plants. RT-qPCR analysis of genes encoding
920 representative markers of the salicylic acid PATHOGENESIS RELATED 1 (PR1), jasmonic
921 acid PLANT DEFENSIN 1.2 (PDF1.2), ethylene PR4 and camalexin [PHYTOALEXIN
922 DEFICIENT 3 (PAD3), CYTOCHROME P450 MONOOXYGENASE 79B2 (CYP79B2)]
923 pathways in *sobir1-12* BIR1 L6 (f) and *bak1*-5 BIR1 L10 (g) plants. In all cases, the same set
924 of replicates from each genotype was used to measure all the genes shown in the graphs.
925 Transcript accumulation was determined in mock-treated (DEX-) versus DEX-treated (DEX+)
926 after 12 days of treatment. Values from biologically independent samples were normalized to
927 the CBP20 internal control, and related to mock-treated plants, set to a value of 1. Data are
928 mean ± SD analyzed by Mann-Whitney test; *, p <0.05. Experiments were repeated at least
929 twice with similar results.

930

931 **Fig. 6.** Phenotypes caused by BAK1-INTERACTING RECEPTOR-LIKE KINASE 1 (BIR1)
932 overexpression are partially rescued in *eds1-2* mutants, but not in *pad4-1* mutants. (a)
933 Morphology of transgenic *eds1-2* BIR1 L1b and *pad4-1* BIR1 L0 mutant plants expressing
934 BIR1 under the control of a dexamethasone (DEX)-inducible 35S promoter. Plants were grown
935 for three weeks on soil and treated with 30 µM DEX to induce BIR1 transcription or mock-
936 treated with H_2O. Plants were photographed after 12 days of the first DEX/ H_2O application.
937 Images from independent transgenic lines are shown in Fig. S7. RT-qPCR analysis of BIR1-
938 coding transcripts in *eds1-2* BIR1 L1b and *pad4-1* BIR1 L0 mutant lines are shown. RT-qPCR
939 analysis of genes encoding the PTI-markers RESPIRATORY BURST OXIDASE HOMOLOG
940 PROTEIN D (RBOHD) and FLG22-INDUCED RECEPTOR-LIKE KINASE 1 (FRK1) in
941 *eds1-2* BIR1 L1b (b) and *pad4-1* BIR1 L0 (c) plants. RT-qPCR analysis of genes encoding
942 representative markers of the salicylic acid PATHOGENESIS RELATED 1 (PR1), jasmonic
943 acid PLANT DEFENSIN 1.2 (PDF1.2), ethylene PR4 and camalexin [PHYTOALEXIN

944 DEFICIENT 3 (PAD3), CYTOCHROME P450 MONOOXYGENASE 79B2 (CYP79B2)]
945 pathways in *eds1-2* BIR1 L1b (d) and *pad4-1* BIR1 L0 (e) plants. In all cases, the same set of
946 replicates from each genotype was used to measure all the genes shown in the graphs. Transcript
947 accumulation was determined in mock-treated (DEX-) versus DEX-treated (DEX+) after 12
948 days of treatment. Values from biologically independent samples were normalized to the
949 CBP20 internal control, and related to mock-treated plants, set to a value of 1. Data are mean ±
950 SD analyzed by Mann-Whitney test; *, p <0.05. Experiments were repeated at least twice with
951 similar results.

952

953 **Fig. 7.** Phenotypes caused by BAK1-INTERACTING RECEPTOR-LIKE KINASE 1 (BIR1)
954 overexpression are independent of salicylic acid (SA)-mediated signaling pathways. (a)
955 Morphology of transgenic *sid2-2* BIR1 (L5) and *eds5-3* BIR1 (L10) mutant plants expressing
956 BIR1 under the control of a dexamethasone (DEX)-inducible 35S promoter. Plants were grown
957 for three weeks on soil and treated with 30 µM DEX to induce BIR1 transcription or mock-
958 treated with H_2O. Plants were photographed after 12 days of the first DEX/ H_2O application.
959 Images from independent transgenic lines are shown in Fig. S7a, b. RT-qPCR analysis of genes
960 encoding BIR1 and representative markers of the salicylic acid PATHOGENESIS RELATED
961 1 (PR1), jasmonic acid PLANT DEFENSIN 1.2 (PDF1.2), ethylene PR4 and camalexin
962 [PHYTOALEXIN DEFICIENT 3 (PAD3), CYTOCHROME P450 MONOOXYGENASE
963 79B2 (CYP79B2)] pathways in *sid2-2* BIR1 (L5) (b) and *eds5-3* BIR1 (L10) (c) mutant lines.
964 In all cases, the same set of replicates from each genotype was used to measure all the genes
965 shown in the graphs. Transcript accumulation was determined in mock-treated (DEX-) versus
966 DEX-treated (DEX+) after 12 days of treatment. Values from biologically independent samples
967 were normalized to the CBP20 internal control, and related to mock-treated plants, set to a value
968 of 1. Data are mean ± SD analyzed by Mann-Whitney test; *, p <0.05. Experiments were
969 repeated at least twice with similar results. (d) Tentative working model for BIR1 homeostasis.
970 SA-mediated transcription of BIR1 is regulated by RNA-directed DNA methylation (RdDM)
971 and post-transcriptional RNA silencing (PTGS) (Guzman-Benito *et al.*, 2019). In these
972 conditions, BIR1 induction interferes with pattern-triggered immunity (PTI) gene expression
973 and plasmodesmata (PD) callose deposition triggered by various elicitors (flg22, nlp20,
974 dsRNA). Loss of BIR1 regulation leads to constitutive BIR1 induction at non-physiological
975 levels that cause SA-independent up-regulation of immune and hormone genes. BIR1
976 overexpression is sensed by one or several TOLL/INTERLEUKIN RECEPTOR 1 (TIR1)-

977 containing nucleotide-binding domain leucine-rich repeat receptors (TNLs), of which
978 CONSTITUTIVE SHADE AVOIDANCE 1 (CSA1) is a plausible candidate, to promote
979 PAD4-independent effector triggered immunity (ETI)-type cell death that requires
980 ENHANCED DISEASE SUSCEPTIBILITY 1 (EDS1) and SUPPRESSOR OF BIR1-1
981 (SOBIR1).

982 **Supporting information**

983 Additional supporting information may be found in the online version of this article

984

985 **Supporting methods**

986 **Methods S1.** RNA and protein analyses.

987 **Methods S2.** Gene expression analyses.

988 **Methods S3.** Analyses of reactive oxygen species (ROS), ethylene, plasmodesmata callose
989 deposition and dexamethasone (DEX) treatments.

990

991 **Supporting figures**

992 **Fig. S1.** Transcriptomic profiling of BAK1-INTERACTING RECEPTOR-LIKE KINASE 1
993 (BIR1) expressing transgenic lines.

994 **Fig. S2.** Transcriptomic profiling of dexamethasone (DEX)-treated wild-type Col-0 plants.

995 **Fig. S3.** Enrichment analysis of Kyoto Encyclopedia of Genes and Genomes (KEGG) pathways
996 using RNA-Seq data.

997 **Fig. S4.** Differential expression of receptor-like protein (RLP)-coding genes in BAK1-
998 INTERACTING RECEPTOR-LIKE KINASE 1 (BIR1) overexpressing plants.

999 **Fig. S5.** Differential expression of cysteine-rich receptor-like kinase (CRK)-coding genes in
1000 BAK1-INTERACTING RECEPTOR-LIKE KINASE 1 (BIR1) overexpressing plants.

1001 **Fig. S6.** Differential expression of cell-surface pattern recognition receptors (PRR)-coding
1002 genes in BAK1-INTERACTING RECEPTOR-LIKE KINASE 1 (BIR1) overexpressing plants.

1003 **Fig. S7**. Differential expression of calcium-dependent protein kinases (CPK)- and
1004 HETEROTRIMERIC G PROTEIN-coding genes in BAK1-INTERACTING RECEPTOR-
1005 LIKE KINASE 1 (BIR1) overexpressing plants.

1006 **Fig. S8.** Morphological and growth defects in BAK1-INTERACTING RECEPTOR-LIKE
1007 KINASE 1 (BIR1) overexpressing plants of different immune mutant genetic backgrounds.

1008

1009 **Supporting tables**

1010 **Table S1.** List of primers

1011 **Table S2.** List of expressed genes.

1012 **Table S3.** List of differentially expressed genes (DEG. padjust value < 0.05).

1013 **Table S4.** List of differentially expressed genes (DEG. |Log2fold change > 1| padjust value <
1014 0.01).

1015 **Table S5.** Enrichment analysis of Gene Ontology (GO) terms.

1016 **Table S6.** Kyoto Encyclopedia of Genes and Genomes (KEGG) pathway enrichment analysis.

1017 **Table S7.** List of differentially expressed genes (DEG. padjust value < 0.05) within functional
1018 categories.

1019 **Table S8**. Statistical analysis of enrichment of functional gene groups in plants overexpressing
1020 BIR1 after 12 days of DEX treatment relative to non-expressing controls using Two-tailed
1021 Fisher's exact tests.

1022

1023

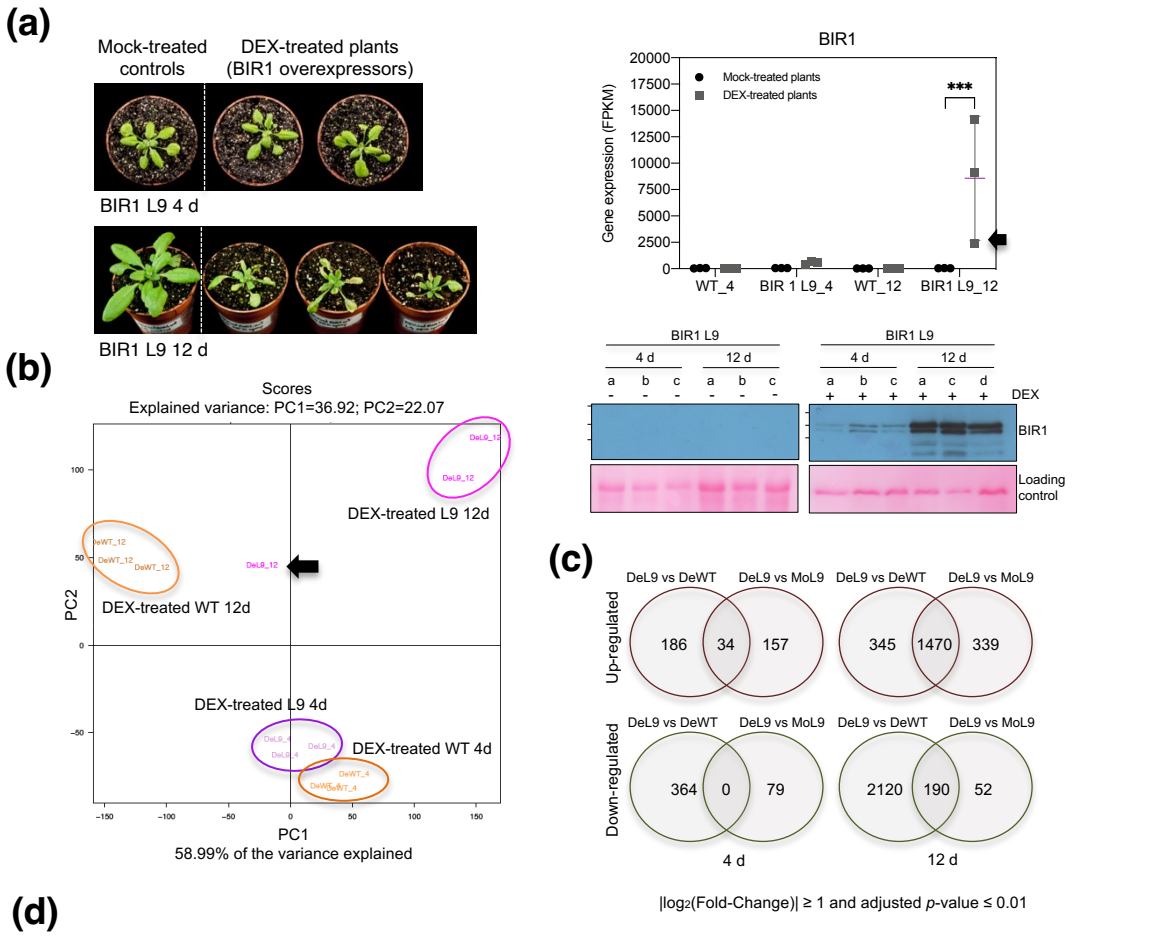

Fig. 1. Transcriptional reprogramming associated with BAK1-INTERACTING RECEPTOR-LIKE KINASE 1 (BIR1) induction in Arabidopsis. (a) Morphology of representative BIR1 transgenic Arabidopsis plants (line 9, L9) under the control of a dexamethasone (DEX)-inducible 35S promoter used for RNA-Seq experiments. Samples were collected after 4 or 12 days of 30 µM DEX treatment. H_2O-treated plants were used as controls. Relative expression of the BIR1-coding gene based on the number of Fragments Per Kilobase of transcript sequence per Millions of base-pairs sequenced (FPKM) (top) and Western blot using anti-mCherry antibody (bottom) in samples used for RNA-Seq. Significant differences between DEX- and mock-treated samples were analyzed using two-way ANOVA followed by Sidak´s multiple comparison test; ***, adjusted *p*-value < 0.001. (b) Principal component analysis (PCA) of RNA-Seq data. The PCA was performed using normalized RNA-Seq data of differentially expressed genes (DEGs) between BIR1 L9 and wild-type (WT) plants after 4 and 12 days of DEX treatment (DeL9_vs DeWT_). Each biological replicate is represented in the score plot. The variance explained by each component (%) is given in parentheses. The sample (DeL9_12b) with differential expression within the DEX-treated L9 group is indicated with black arrows in (a) and (b). (c) Number of up-or down-regulated transcripts, with a $|\log_2(\text{Fold-Change})| \geq 1$ and adjusted *p*-value ≤0.01, in each pairwise comparison is indicated. (d) Scatterplot of selected gene ontology (GO) terms of DEGs. GO terms between WT and BIR1 L9 plants at 4 and 12 days after DEX-treatment (DeL9_ vs DeWT_) are shown. Dot size represents the count of different genes and the color indicates significance of the term enrichment. GO terms with adjusted *p*-value < 0.05 are significantly enriched. The kinase term (indicated by an arrow) was exclusively assigned to BIR1 L9 plants. WT, wild-type Col-0; L9, BIR1 L9 transgenic plants; De, DEX-treated plants; Mo, Mock-treated plants; _4, 4 days of treatment; _12, 12 days of treatment.

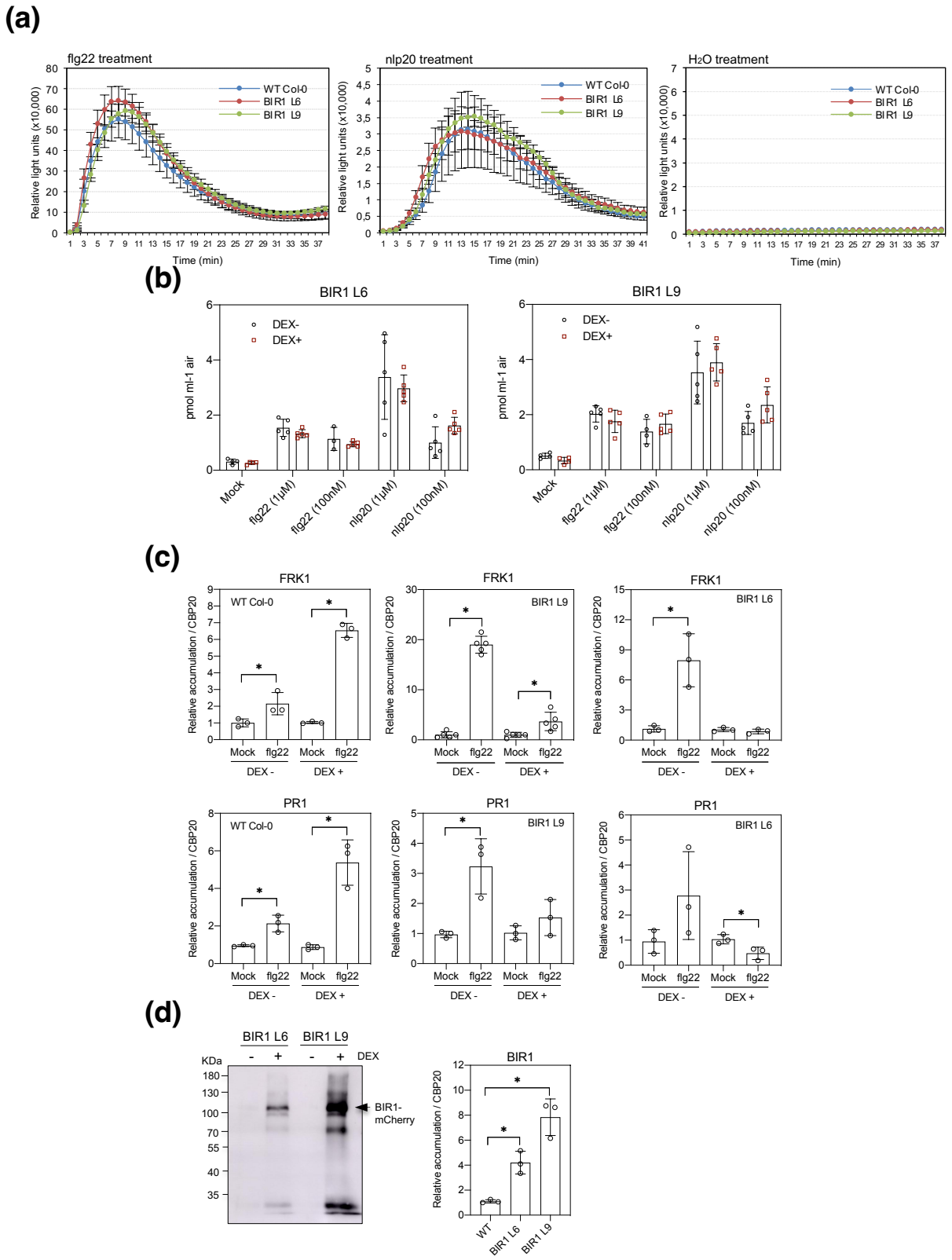

Fig. 2. Effect of BAK1-INTERACTING RECEPTOR-LIKE KINASE 1 (BIR1) induction on immune responses triggered by flg22 and nlp20 treatments. (a) Over time production of reactive oxygen species (ROS) in dexamethasone (DEX)-treated wild-type (WT) and BIR1 L6 and L9 transgenic plants after elicitation of Arabidopsis leaf disks with 1 µM flg22 (left), 1 µM nlp20 (middle) or H_2O (right). Bars represent means ± SD of relative fluorescence units. (b) Ethylene accumulation in BIR1 L6 and L9 transgenic plants after treatment with H_2O (mock), flg22 and nlp20 at 1 µM or 100 nM concentration as indicated. Bars represent average values ± SD. Within each elicitor/mock treatment, differences between DEX-treated (DEX+) and controls (DEX-) were analyzed by two-way ANOVA followed by Sidak´s multiple comparison test. (c) RT-qPCR analysis of the genes encoding the PTI-markers FLG22-INDUCED RECEPTOR-LIKE KINASE 1 (FRK1) and PATHOGENESIS RELATED 1 (PR1) at 45 min after treatment with H_2O (mock) or 1 µM flg22, and determined in DEX-treated (DEX+) versus non-treated (DEX-) samples. (d) Immunoprecipitation of mCherry-BIR1 fusion proteins, indicated with an arrowhead, from samples of BIR1 L6 and L9 plants used in (a) and (b) (left), and RT-qPCR analysis of BIR1-coding transcripts in DEX-treated (DEX+) samples of BIR1 L6 and L9 plants used in (c) (right). In all cases, RT-qPCR values from biologically independent samples were normalized to the CBP20 internal control, and related to H_2O (mock)-treated plants, set to a value of 1. Data are means ± SD analyzed by Kruskal-Wallis test; *, adjusted *p*-value <0.05. Experiments were repeated three times with similar results.

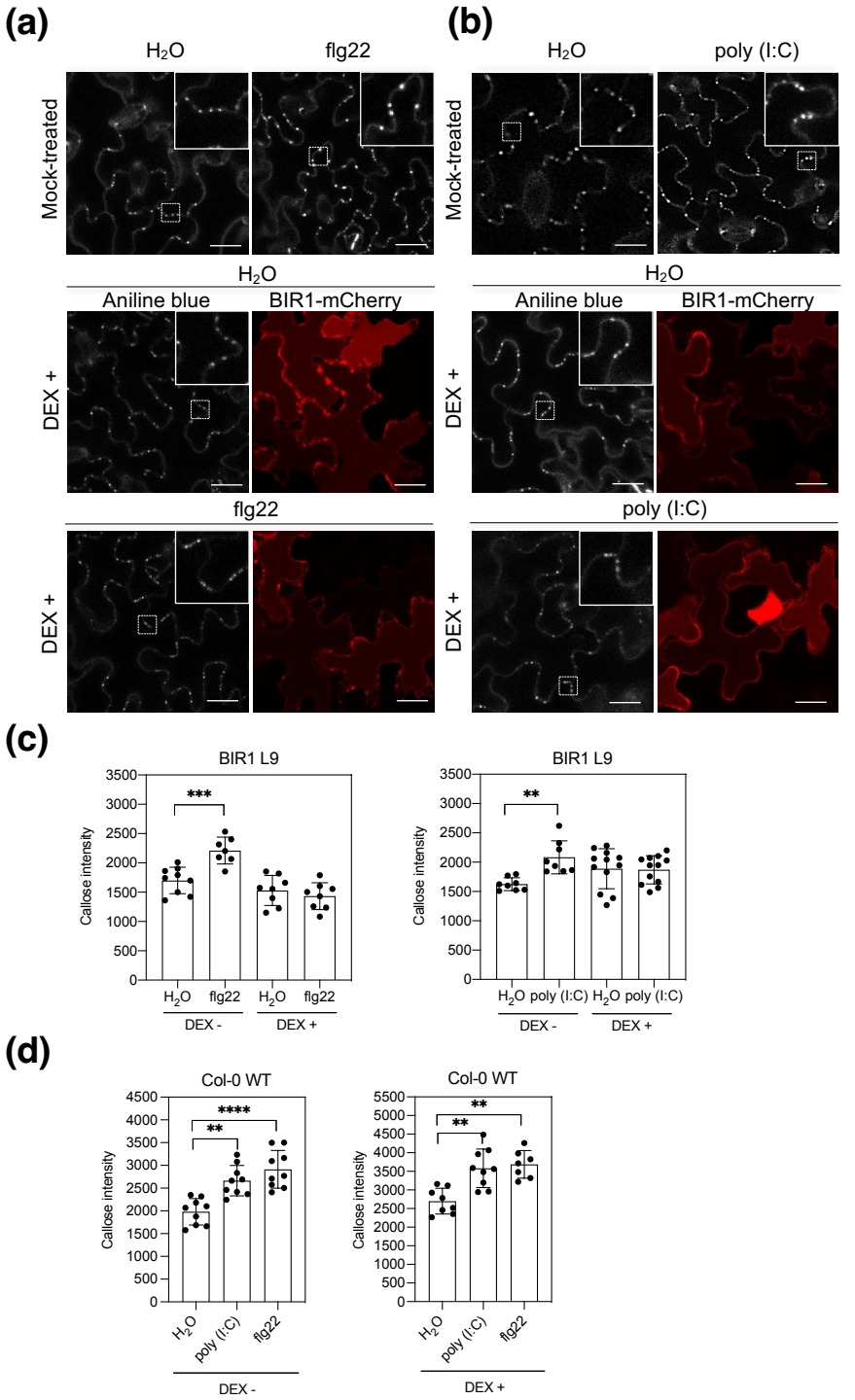

Fig. 3. BAK1-INTERACTING RECEPTOR-LIKE KINASE 1 (BIR1) induction inhibits flg22- and poly(I:C)-triggered callose accumulation at plasmodesmata (PD). Callose spots at PD were visualized upon aniline blue staining of epidermal cells in response to bacterial flg22 (a) or poly(I:C) (b) in BIR1 L9 transgenic Arabidopsis plants. Plants were previously sprayed with 30 µM dexamethasone (DEX) for three days to elicit BIR1 expression. Mock-treated plants were used as non BIR1-expressing controls (top panels). Photographs were taken 30 minutes after treatment with H_2O (control) or 1 µM flg22 or 50 ng/µl of poly(I:C). BIR1-mCherry fluorescence in DEX-treated BIR1 L9 plants was confirmed within the same images. Inlays show enlargements of the areas within the dashed boxes. Scale bar, 10 µm. (c) Relative PD callose content in flg22/poly(I:C)-treated and H_2O (control)-treated leaves from BIR1 L9 plants previously treated with or without DEX as indicated. d) Callose content at PD in control (DEX -) and DEX-treated wild-type (WT) plants in response to H_2O and poly (I:C) is shown. In all cases, black dots represent the mean values of callose intensities in individual PD (>100) measured in three leaf discs taken from at least three independent biological replicates per each treatment. Significant differences between samples were analyzed by Kruskal-Wallis test or by one-way ANOVA followed by Tukey's multiple comparison test; ****, adjusted *p*-value <0.0001, ***, <0.001, **, <0.01. Experiments were repeated twice with similar results.

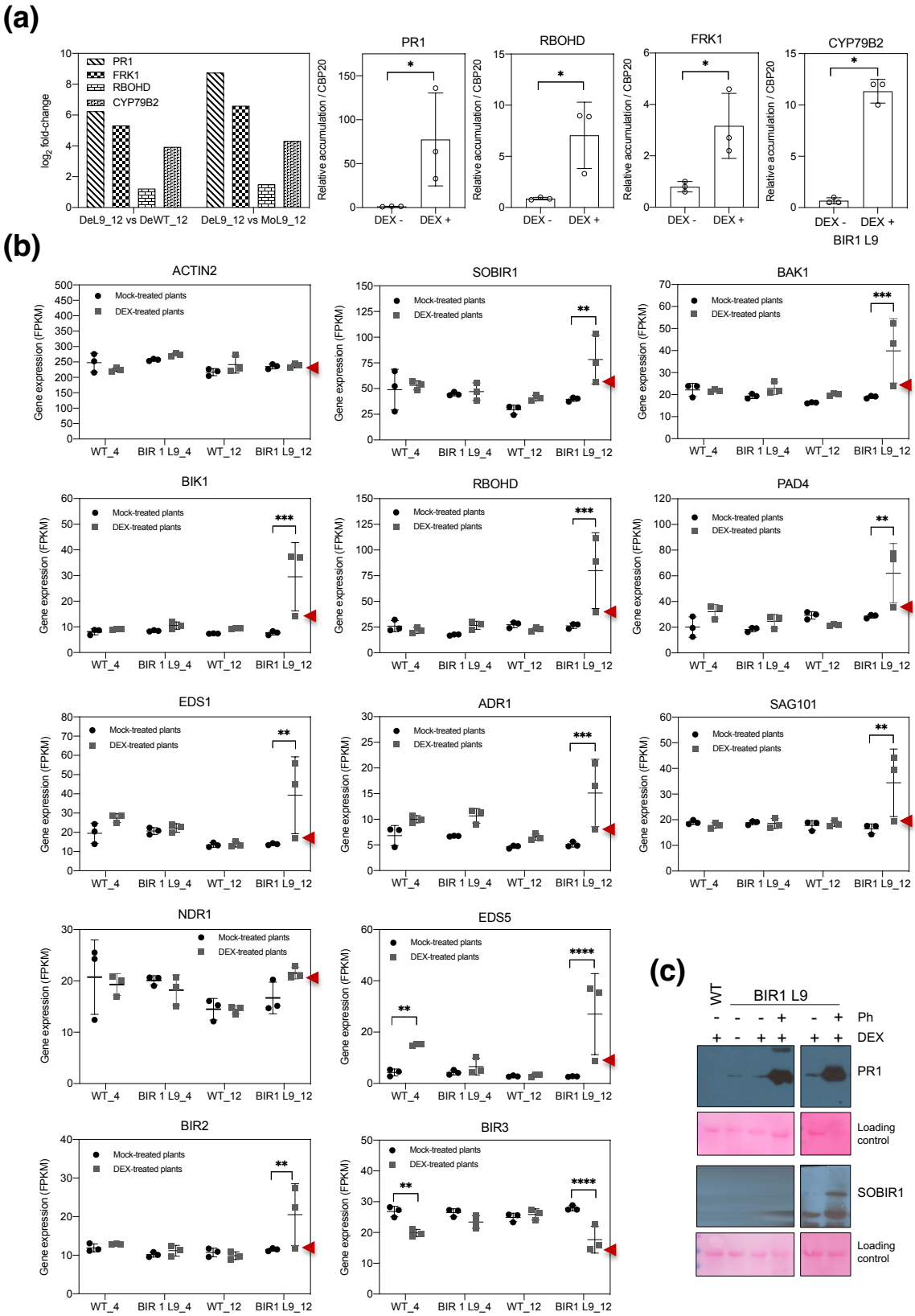

Fig. 4. BAK1-INTERACTING RECEPTOR-LIKE KINASE 1 (BIR1) overexpression leads to the transcriptional activation of pattern-triggered immunity (PTI)-associated co-receptors and effector-triggered immunity (ETI) regulators. (a) Validation of the RNA-Seq results. Expression of markers encoded by selected BIR1-responsive differentially expressed genes (DEGs) after 12 days of dexamethasone (DEX) treatment based on fold-change values (log_2 DeL9_12/DeWT_12 and log_2 DeL9_12/MoL9_12 as indicated) was confirmed by RT-qPCR. Values from biologically independent samples were normalized to the CBP20 internal control, and related to untreated (DEX-) plants, set to a value of 1. Data are mean ± SD analyzed by Mann-Whitney test; *, p <0.05. (b) Relative expression of selected genes encoding PTI/ETI-markers based on the number of Fragments Per Kilobase of transcript sequence per Millions of base-pairs sequenced (FPKM) in each of the three independent samples per condition used for RNA-Seq. Actin expression is shown as control. Note that the expression levels of each individual replicate within the DEX-treated BIR1 L9_12 group mirror the abundance of BIR1 transcripts in each replicate. DeL9_12b is indicated by a red arrow. Significant differences between mock-treated and DEX-treated samples were analyzed using two-way ANOVA followed by Sidak´s multiple comparison test; ****, adjusted p-value < 0.0001, *** < 0.001, **< 0.01. WT, wild-type Col-0; L9, BIR1 L9 transgenics; _4d, 4 days of treatment; _12d, 12 days of treatment. (c) Western blot analysis of SUPPRESSOR OF BIR1-1 (SOBIR1) and PATHOGENESIS RELATED 1 (PR1) using specific antibodies in two independent sets of BIR1 L9 samples. Plants were mock-treated (-) or DEX-treated (+) for 12 days. The presence (+) or absence (-) of morphological phenotypes (Ph) in each sample is indicated. Protein loading control by Ponceau S is shown.

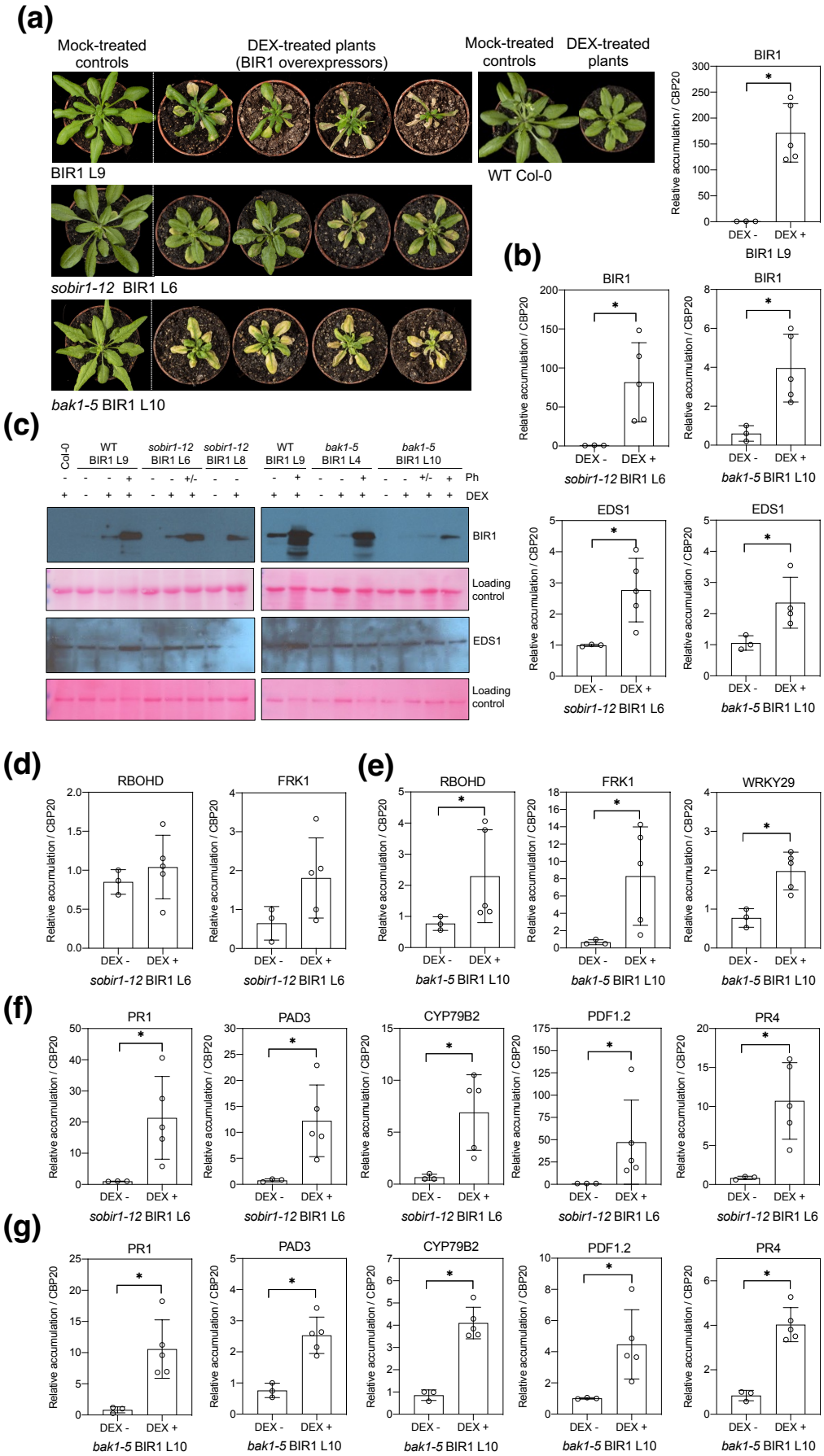
(a)
Mock-treated controls
DEX-treated plants (BIR1 overexpressors)
Mock-treated controls
DEX-treated plants
BIR1 L9
WT Col-0
sobir1-12 BIR1 L6
bak1-5 BIR1 L10
BIR1
Relative accumulation / CBP20
DEX -
DEX +
BIR1 L9
(b)
sobir1-12 BIR1 L6
bak1-5 BIR1 L10
EDS1
(c)
Col-0
WT BIR1 L9
sobir1-12 BIR1 L6
sobir1-12 BIR1 L8
WT BIR1 L9
bak1-5 BIR1 L4
bak1-5 BIR1 L10
Ph
DEX
BIR1
Loading control
EDS1
Loading control
(d)
RBOHD
FRK1
sobir1-12 BIR1 L6
(e)
RBOHD
FRK1
WRKY29
bak1-5 BIR1 L10
(f)
PR1
PAD3
CYP79B2
PDF1.2
PR4
sobir1-12 BIR1 L6
(g)
PR1
PAD3
CYP79B2
PDF1.2
PR4
bak1-5 BIR1 L10

Fig. 5. Phenotypes caused by BAK1-INTERACTING RECEPTOR-LIKE KINASE 1 (BIR1) overexpression are partially rescued in *sobir1-12* mutants, but not in a *bak1-5* mutant. Morphology of transgenic *sobir1-12* BIR1 L6 and *bak1*-5 BIR1 L10 mutant plants expressing BIR1 under the control of a dexamethasone (DEX)-inducible 35S promoter. Transgenic BIR1 L9 plants in the wild-type (WT) Col-0 background are shown as a reference. Plants were grown for three weeks on soil and treated with 30 µM dexamethasone (DEX) to induce BIR1 transcription or mock-treated with H_2O. Non-transgenic WT Col-0 plants are shown as controls. Plants were photographed after 12 days of the first DEX/ H_2O application. Images from independent transgenic lines are shown in Fig. S7. RT-qPCR analysis of *BIR1* transcripts in BIR1 L9 plants are shown. b) RT-qPCR analysis of BIR1 and ENHANCED DISEASE SUSCEPTIBILITY 1 (EDS1) transcripts in *sobir1-12* BIR1 L6 and *bak1*-5 BIR1 L10 plants. c) Western blot analysis of BIR1 and EDS1 proteins with specific antibodies in WT BIR1 L9 and two independent lines of *sobir1-12* BIR1 (L6, L8) and *bak1*-5 BIR1 (L4, L10). Plants were mock-treated (-) or DEX-treated (+) for 12 days as indicated. The presence (+) or absence (-) of morphological phenotypes (Ph) in each sample is indicated. Protein loading control by Ponceau S is shown. RT-qPCR analysis of genes encoding the PTI-markers RESPIRATORY BURST OXIDASE HOMOLOG PROTEIN D (RBOHD), FLG22-INDUCED RECEPTOR-LIKE KINASE 1 (FRK1) or WRKY DNA-BINDING PROTEIN 29 (WRKY29) in *sobir1-12* BIR1 L6 (d) and *bak1*-5 BIR1 L10 (e) plants. RT-qPCR analysis of genes encoding representative markers of the salicylic acid PATHOGENESIS RELATED 1 (PR1), jasmonic acid PLANT DEFENSIN 1.2 (PDF1.2), ethylene PR4 and camalexin [PHYTOALEXIN DEFICIENT 3 (PAD3), CYTOCHROME P450 MONOOXYGENASE 79B2 (CYP79B2)] pathways in *sobir1-12* BIR1 L6 (f) and *bak1*-5 BIR1 L10 (g) plants. In all cases, the same set of replicates from each genotype was used to measure all the genes shown in the graphs. Transcript accumulation was determined in mock-treated (DEX-) versus DEX-treated (DEX+) after 12 days of treatment. Values from biologically independent samples were normalized to the CBP20 internal control, and related to mock-treated plants, set to a value of 1. Data are mean ± SD analyzed by Mann-Whitney test; *, $p < 0.05$. Experiments were repeated at least twice with similar results.

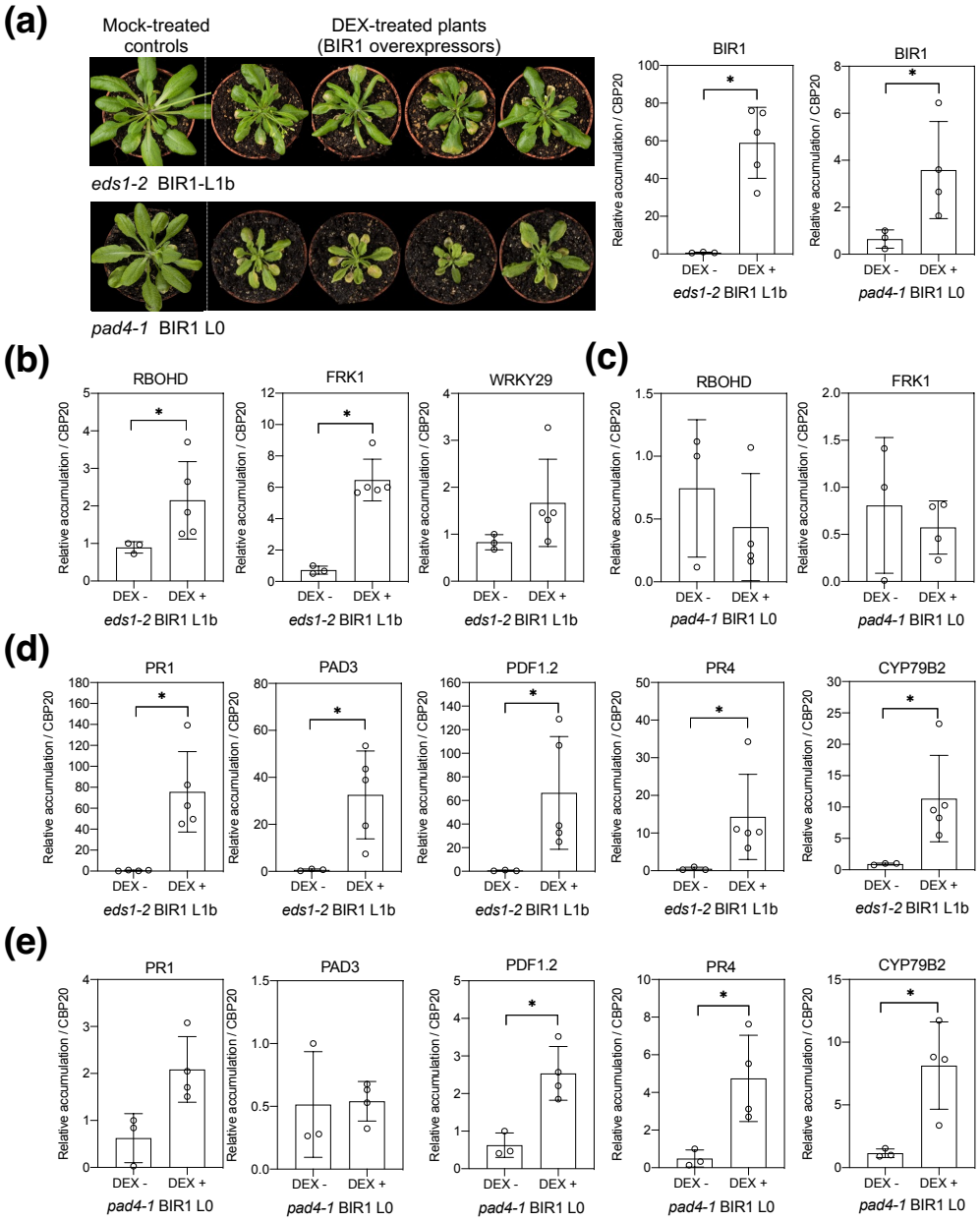

Fig. 6. Phenotypes caused by BAK1-INTERACTING RECEPTOR-LIKE KINASE 1 (BIR1) overexpression are partially rescued in *eds1-2* mutants, but not in *pad4-1* mutants. (a) Morphology of transgenic *eds1-2* BIR1 L1b and *pad4-1* BIR1 L0 mutant plants expressing BIR1 under the control of a dexamethasone (DEX)-inducible 35S promoter. Plants were grown for three weeks on soil and treated with 30 µM DEX to induce BIR1 transcription or mock-treated with H_2O. Plants were photographed after 12 days of the first DEX/ H_2O application. Images from independent transgenic lines are shown in Fig. S7. RT-qPCR analysis of BIR1-coding transcripts in *eds1-2* BIR1 L1b and *pad4-1* BIR1 L0 mutant lines are shown. RT-qPCR analysis of genes encoding the PTI-markers RESPIRATORY BURST OXIDASE HOMOLOG PROTEIN D (RBOHD) and FLG22-INDUCED RECEPTOR-LIKE KINASE 1 (FRK1) in *eds1-2* BIR1 L1b (b) and *pad4-1* BIR1 L0 (c) plants. RT-qPCR analysis of genes encoding representative markers of the salicylic acid PATHOGENESIS RELATED 1 (PR1), jasmonic acid PLANT DEFENSIN 1.2 (PDF1.2), ethylene PR4 and camalexin [PHYTOALEXIN DEFICIENT 3 (PAD3), CYTOCHROME P450 MONOOXYGENASE 79B2 (CYP79B2)] pathways in *eds1-2* BIR1 L1b (d) and *pad4-1* BIR1 L0 (e) plants. In all cases, the same set of replicates from each genotype was used to measure all the genes shown in the graphs. Transcript accumulation was determined in mock-treated (DEX-) versus DEX-treated (DEX+) after 12 days of treatment. Values from biologically independent samples were normalized to the CBP20 internal control, and related to mock-treated plants, set to a value of 1. Data are mean ± SD analyzed by Mann-Whitney test; *, $p < 0.05$. Experiments were repeated at least twice with similar results.

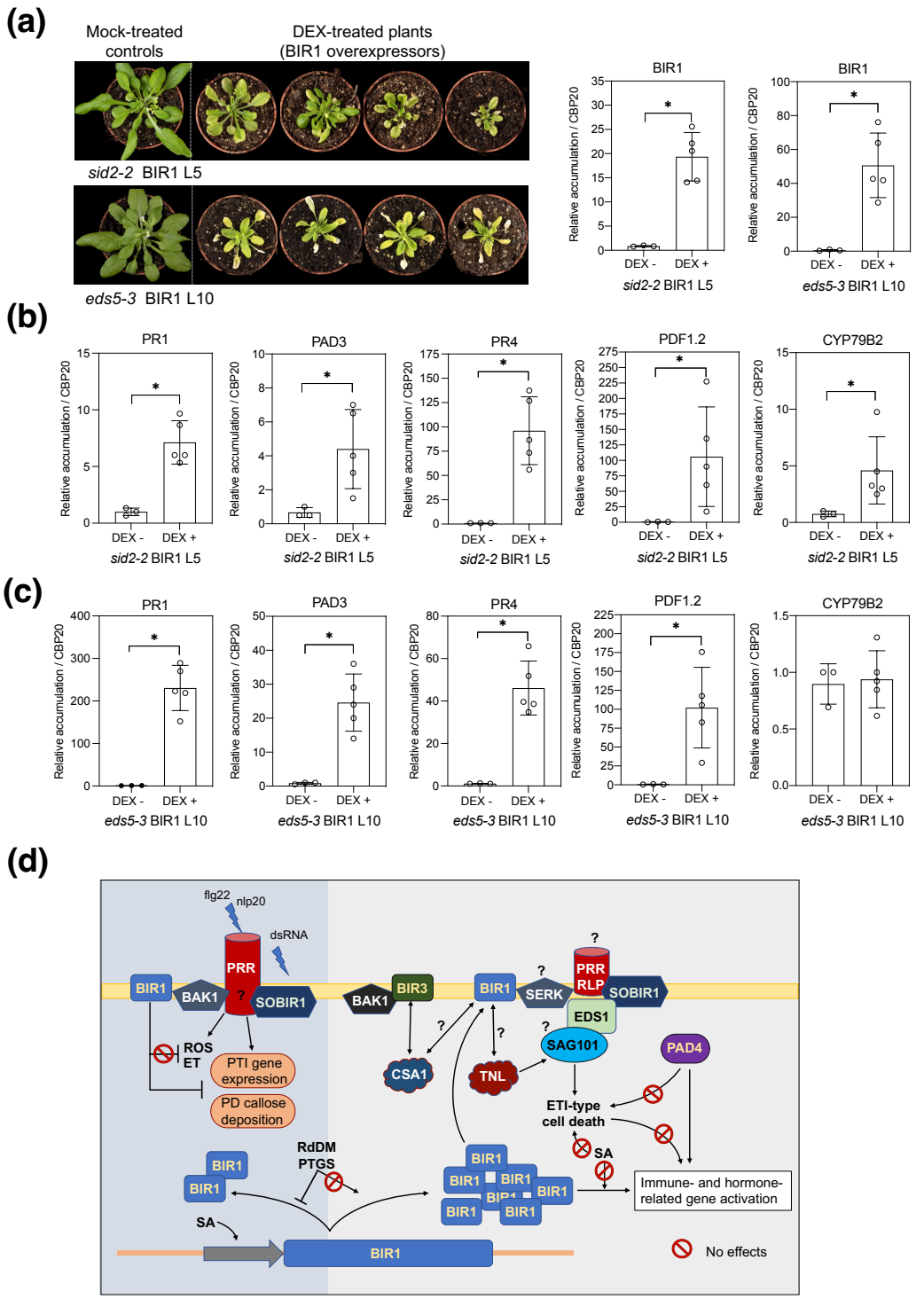

Fig. 7. Phenotypes caused by BAK1-INTERACTING RECEPTOR-LIKE KINASE 1 (BIR1) overexpression are independent of salicylic acid (SA)-mediated signaling pathways. (a) Morphology of transgenic *sid2-2* BIR1 (L5) and *eds5-3* BIR1 (L10) mutant plants expressing BIR1 under the control of a dexamethasone (DEX)-inducible 35S promoter. Plants were grown for three weeks on soil and treated with 30 µM DEX to induce BIR1 transcription or mock-treated with H_2O. Plants were photographed after 12 days of the first DEX/ H_2O application. Images from independent transgenic lines are shown in Fig. S7a, b. RT-qPCR analysis of genes encoding BIR1 and representative markers of the salicylic acid PATHOGENESIS RELATED 1 (PR1), jasmonic acid PLANT DEFENSIN 1.2 (PDF1.2), ethylene PR4 and camalexin [PHYTOALEXIN DEFICIENT 3 (PAD3), CYTOCHROME P450 MONOOXYGENASE 79B2 (CYP79B2)] pathways in *sid2-2* BIR1 (L5) (b) and *eds5-3* BIR1 (L10) (c) mutant lines. In all cases, the same set of replicates from each genotype was used to measure all the genes shown in the graphs. Transcript accumulation was determined in mock-treated (DEX-) versus DEX-treated (DEX+) after 12 days of treatment. Values from biologically independent samples were normalized to the CBP20 internal control, and related to mock-treated plants, set to a value of 1. Data are mean ± SD analyzed by Mann-Whitney test; *, p <0.05. Experiments were repeated at least twice with similar results. (d) Tentative working model for BIR1 homeostasis. SA-mediated transcription of BIR1 is regulated by RNA-directed DNA methylation (RdDM) and post-transcriptional RNA silencing (PTGS) (Guzman-Benito *et al.*, 2019). In these conditions, BIR1 induction interferes with pattern-triggered immunity (PTI) gene expression and plasmodesmata (PD) callose deposition triggered by various elicitors (flg22, nlp20, dsRNA). Loss of BIR1 regulation leads to constitutive BIR1 induction at non-physiological levels that cause SA-independent up-regulation of immune and hormone genes. BIR1 overexpression is sensed by one or several TOLL/INTERLEUKIN RECEPTOR 1 (TIR1)-containing nucleotide-binding domain leucine-rich repeat receptors (TNLs), of which CONSTITUTIVE SHADE AVOIDANCE 1 (CSA1) is a plausible candidate, to promote PAD4-independent effector triggered immunity (ETI)-type cell death that requires ENHANCED DISEASE SUSCEPTIBILITY 1 (EDS1) and SUPPRESSOR OF BIR1-1 (SOBIR1).

New Phytologist Supporting Information

Article title:

The receptor-like kinase BIR1 inhibits elicitor-induced plasmodesmata callose deposition and PTI gene expression and requires EDS1 and SOBIR1 to cause dose-dependent cell-death in Arabidopsis

Irene Guzmán-Benito[1], Carmen Robinson[1,2], Chenlei Hua[3], Ana Rocio Sede[4], Laura Elvira-González[4], Isabel Punzón[1], Manfred Heinlein[4], Thorsten Nürnberger[3,5], César Llave[1]*

[1]Centro de Investigaciones Biológicas Margarita Salas. Consejo Superior de Investigaciones Científicas, Ramiro de Maeztu 9, 28040 Madrid, Spain; [2]Doctorado en Biotecnología y Recursos Genéticos de Plantas y Microorganismos Asociados, Universidad Politécnica de Madrid, 28040-Madrid, Spain; [3]Department of Plant Biochemistry, Center of Plant Molecular Biology (ZMBP), University of Tübingen, Tübingen, Germany; [4]Institut de Biologie Moléculaire des Plantes, CNRS, Université de Strasbourg, 67000 Strasbourg, France; [5]Department of Biochemistry, University of Johannesburg, Johannesburg, South Africa.

The following Supporting Information is available for this article:

Methods S1. RNA and protein analyses.

Methods S2. Gene expression analyses.

Methods S3. Reactive oxygen species (ROS), ethylene, plasmodesmata callose deposition and dexamethasone (DEX) treatments.

Fig. S1. Transcriptomic profiling of BAK1-INTERACTING RECEPTOR-LIKE KINASE 1 (BIR1) expressing transgenic lines.

Fig. S2. Transcriptomic profiling of dexamethasone (DEX)-treated wild-type Col-0 plants.

Fig. S3. Enrichment analysis of Kyoto Encyclopedia of Genes and Genomes (KEGG) pathways using RNA-Seq data.

Fig. S4. Differential expression of receptor-like protein (RLP)-coding genes in BAK1-INTERACTING RECEPTOR-LIKE KINASE 1 (BIR1) overexpressing plants.

Fig. S5. Differential expression of cysteine-rich receptor-like kinase (CRK)-coding genes in BAK1-INTERACTING RECEPTOR-LIKE KINASE 1 (BIR1) overexpressing plants.

Fig. S6. Differential expression of cell-surface pattern recognition receptors (PRR)-coding genes in BAK1-INTERACTING RECEPTOR-LIKE KINASE 1 (BIR1) overexpressing plants.

Fig. S7. Differential expression of calcium-dependent protein kinases (CPK)- and HETEROTRIMERIC G PROTEIN-coding genes in BAK1-INTERACTING RECEPTOR-LIKE KINASE 1 (BIR1) overexpressing plants.

Fig. S8. Morphological and growth defects in BAK1-INTERACTING RECEPTOR-LIKE KINASE 1 (BIR1) overexpressing plants of different immune mutant genetic backgrounds.

Table S1. List of primers

Table S2. List of expressed genes.

Table S3. List of differentially expressed genes (DEG. padjust value < 0.05).

Table S4. List of differentially expressed genes (DEG. |Log2fold change > 1| padjust value < 0.01).

Table S5. Enrichment analysis of Gene Ontology (GO) terms.

Table S6. Kyoto Encyclopedia of Genes and Genomes (KEGG) pathway enrichment analysis.

Table S7. List of differentially expressed genes (DEG. padjust value < 0.05) within functional categories.

Table S8. Statistical analysis of enrichment of functional gene groups in plants overexpressing BIR1 after 12 days of DEX treatment relative to non-expressing controls using Two-tailed Fisher's exact tests.

57 **Supporting methods**

58

59 **Methods S1. RNA and protein analyses**

60 RNA analysis. Total RNA was extracted using TRIzol reagent (Invitrogen) and treated with
61 DNase I (Invitrogen) following manufacturer's instructions to eliminate genomic DNA traces.
62 One-step quantitative RT-PCR (RT-qPCR) was carried out using Brilliant III Ultra-Fast SYBR
63 Green QRT-PCR Master Mix (Agilent Technologies) in a Rotor-Gene 6000/Rotor-Gene Q real-
64 time PCR machine (Corbett/Qiagen) (Fernandez-Calvino *et al.*, 2016). Relative gene
65 expression was determined using the Delta-delta cycle threshold method and Rotor-Gene 6000
66 Series Software (Corbett). Transcript levels of the target genes were normalized to the transcript
67 levels of the housekeeping gene CBP20 (At5g44200) as a reference gene.

68 Protein analyses. Leaf tissue samples were ground in liquid nitrogen in an Eppendorf tube and
69 homogenized in extraction buffer (65 mM Tris-HCl, pH 8; 3% sodium dodecyl sulfate [SDS];
70 1% ß-mercaptoethanol; 10% glycerol). Samples were diluted in Laemmli buffer, incubated for
71 5 min at 95°C, and loaded onto 10% SDS-PAGE protein gels. After electrophoresis, proteins
72 were blotted onto an ECL nitrocellulose membrane (Amersham-Pharmacia), and detected using
73 commercial horseradish peroxide (HRP)-conjugated secondary antibodies and a
74 chemiluminescent substrate (LiteAblot Plus). Primary and secondary antibodies were diluted
75 according to the manufacturer's recommendations. The RFP-Trap (Chromotek) was used for
76 immunoprecipitation of mCherry-tagged BIR1 protein from Arabidopsis leaves following
77 manufacturer's instruction.

78

79 **Methods S2. Gene expression analyses**

80 RNA and library preparation for transcriptome sequencing. Total RNA was extracted from each
81 sample using the RNeasy plant mini kit (Qiagen) followed by DNase treatment according to
82 manufacturer's instructions. A total of 24 samples, including three biological replicates per
83 treatment, were collected. Each sample consisted of RNA pooled from six individual plants.
84 RNA degradation and contamination were monitored on 1% agarose gels, and BIR1 transcript
85 accumulation was measured by RT-qPCR. The RNA purity and RNA concentration were
86 checked using a Nanodrop spectrophotometer (ThermoFisher Scientific), while the RNA
87 integrity was measured using the Agilent Bioanalyzer 2100 system (Agilent Technologies).
88 Sequencing libraries were generated at NOVOGENE (HK) COMPANY LIMITED (Wan Chai,

89 Hong Kong) (www.novogene.com) using NEBNext® UltraTM RNA Library Prep Kit for
90 Illumina® (New England Biolabs) following manufacturer's recommendations and index codes
91 were added to attribute sequences to each sample. First-strand cDNA from mRNA was
92 synthesized using random hexamer primer and M-MuLV Reverse Transcriptase (RNase H-).
93 Second-strand cDNA synthesis was subsequently performed using DNA Polymerase I and
94 RNase H. NEBNext Adaptors with hairpin loop structure were ligated. In order to select cDNA
95 fragments of preferentially 150~200 bp in length, the library fragments were purified with the
96 AMPure XP system (Beckman Coulter). PCR was done with Phusion High-Fidelity DNA
97 polymerase, Universal PCR primers and Index (X) Primer. PCR products were purified with
98 the AMPure XP system and library quality was assessed on the Agilent Bioanalyzer 2100
99 system. Clustering of the index-coded samples was performed on a cBot Cluster Generation
100 System using the TruSeq PE Cluster Kit v3-cBot-HS (Illumina) according to the manufacturer's
101 recommendations. Finally, paired-end reads were generated via an Illumina PE150 Hiseq
102 platform at NOVOGENE (HK) COMPANY LIMITED.

103 Bioinformatics analysis of RNA-Seq data. Clean reads were obtained by removing adaptor tags
104 and reads containing poly-N and low-quality reads from raw data. Paired-end clean reads were
105 mapped to the Arabidopsis TAIR v10 reference genome using HISAT2 software. To quantify
106 the gene expression levels, HTSeq v0.6.1 was used to calculate the number of mapped reads of
107 each gene and then normalize the results to the expected number of Fragments Per Kilobase of
108 transcript sequence per Millions of base-pairs sequenced (FPKM). Differential expression
109 analysis between groups (three biological replicates per condition) was performed using
110 DESeq2 R package (1.18.0). The resulting *p-value*s were adjusted using the Benjamini and
111 Hochberg's approach for controlling the False Discovery Rate (FDR). Genes with an adjusted
112 *p-value* ≤0.05 found by DESeq2 were deemed as differentially expressed (DEG). Functional
113 classification of DEGs including Gene Ontology (GO) and KEGG was performed. GO
114 enrichment analysis of DEGs was implemented by tGOseq R package, in which gene length
115 bias was corrected. KOBAS software was used to test the statistical enrichment of DEGs in the
116 KEGG database GO terms and KEGG pathways with corrected *p-value* ≤0.05 were considered
117 significantly enriched by DEGs.

118

119 **Methods S3. Reactive oxygen species (ROS), ethylene, plasmodesmata callose deposition**
120 **and dexamethasone (DEX) treatments**

121 ROS and ethylene measurements. The detection of ROS and ethylene was performed as
122 described (Albert *et al.*, 2015; Wan *et al.*, 2019). Approximately 3-4 week-old BIR1 L9 or WT
123 Arabidopsis plants were treated with 30 µM dexamethasone (DEX) (H_2O was used as control)
124 for 4 days at 24 h intervals and leaves were then cut into pieces and left floating on H_2O
125 overnight before measurement. For ROS assays, leaf pieces were analyzed in a 96-well plate
126 containing 20 µM L-012 (Wako Pure Chemical Industries Ltd) and 2 µg ml^{-1} peroxidase.
127 Luminescence was measured both before (background) and over 1 h following flg22 or nlp20
128 (GenScript Biotech) elicitation or mock treatment using a Mithras LB 940 luminometer
129 (Berthold Technologies). For ethylene measurement, leaf pieces were incubated in 20 mM MES
130 buffer, pH 5.6 and the indicated elicitor (GenScript Biotech). Ethylene accumulation was
131 measured by gas chromatographic analysis (GC-14A) of 1 ml of the air drawn from the closed
132 tube with a syringe after the indicated incubation time. At least three replicates were performed
133 for all treatments.

134 Callose staining. Approximately 3-4 week-old BIR1 L9 or WT Arabidopsis plants were sprayed
135 with 30 µM DEX (H_2O was used as control) for 3-4 days at 24 h intervals and then leaf disks
136 were excised and left floating on H_2O. For callose staining, individual leaf disks were soaked
137 with 0,1% aniline blue solution (in 50 mM potassium phosphate buffer, pH 8.0) containing
138 either 0.5 µg $µl^{-1}$ poly(I:C) (Sigma) or 1 µM flg22 (GenScript Biotech). Leaf disks were further
139 evacuated for 1-2 minutes (< 0.8 pa) in a vacuum desiccator. Aniline blue fluorescence was
140 imaged 30 minutes after poly(I:C)/flg22 or control treatment using a Zeiss LSM 780 confocal
141 laser scanning microscope with ZEN 2.3 software (Carl Zeiss) and using a 405 nm diode laser
142 for excitation and filtering the emission at 475-525 nm. mCherry fluorescence was excited at
143 561 nm filtering the emission at 560-610 nm. 8-bit images were acquired with a Plant-
144 Apochromat 40x/1.4 Oil DIC M27 objective. Callose fluorescence intensity was quantified with
145 ImageJ software (http://rsbweb.nih. gov/ij/) using the plug-in calloseQuant (Huang *et al.*,
146 2022). Callose spots were measured in 3-4 images taken from each leaf disk. If not otherwise
147 mentioned, three leaf discs per plant from three different plants were evaluated for each
148 genotype or condition. Regions of interest (ROIs) selected by calloseQuant were verified
149 visually before measurement. Individual fluorescence intensities that occurred as outliers from
150 the general distribution of fluorescence intensities (<1%) in the sample were excluded from
151 analysis.

152 Dexamethasone (DEX) treatments. DEX (Sigma) was dissolved in 100% ethanol to make a 30
153 mM DEX stock solution which was stored at –20°C in a light-tight vial. For the time course

experiments monitoring BIR1 expression, Col-0 wild-type (controls) and transgenic BIR1 L9 and L6 plants were grown for 3 weeks in soil and sprayed at 24 h intervals with DEX at 30 µM as indicated {McNellis, 1998 #2330}. At this concentration, plants display optimal induction of the transgene {Guzman-Benito, 2019 #2456}. For RNA-seq, samples were harvested after 4 or 12 days of DEX treatments, before the appearance of cell-death-like symptoms. For gene expression assays in mutant backgrounds, plants were collected by the time symptoms appeared, which normally occurred after 10-14 days of DEX treatments. After 4 and 12 days of treatments BIR1 was produced at physiological and non-physiological levels, respectively. WT plants treated with DEX for 4 days exhibit normal growth and development, whereas a slight growth retardation was observed in DEX-treated WT plants after 12 days of DEX treatment **(Fig. 5a)**.

Supporting figures

Fig. S1. Transcriptomic profiling of BAK1-INTERACTING RECEPTOR-LIKE KINASE 1 (BIR1) expressing transgenic lines. (a) Principal component analysis (PCA) of RNA-Seq data. The PCA was performed using normalized RNA-Seq data of differentially expressed genes (DEGs) between dexamethasone (DEX)-treated and mock-treated transgenic BIR1 L9 plants after 4 and 12 days of treatment (DeL9_vs MoL9_). Each biological replicate is represented in the score plot. The variance explained by each component (%) is given in parentheses. The sample (DeL9_12b) with differential expression within the DEX-treated L9 group is indicated with a black arrow. (b) Number of up-or down-regulated transcripts, with a $|\log_2(\text{Fold-Change})| \geq 1$ and adjusted p-value ≤ 0.05, in each pairwise comparison as indicated. (c) Volcano plots showing the distribution of DEGs (adjusted p-value ≤ 0.05). The x-axis shows the fold change in gene expression between samples, and y-axis shows the statistical significance of the differences. Significantly up- and down-regulated genes are highlighted in red and green, respectively. Genes that are not differentially regulated are in blue. (d) Scatterplot of selected gene ontology (GO) terms of DEGs. GO terms between wild-type (WT) and BIR1 L9 plants at 4 and 12 days after DEX-treatment (DeL9_ vs MoL9_) are shown. Dot size represents the count of different genes and the color indicates significance of the term enrichment. GO terms with adjusted p-value < 0.05 are significantly enriched. The kinase term (indicated by an arrow) was

186 exclusively assigned to BIR1 L9 plants. WT, wild-type Col-0; L9, BIR1 L9 transgenic plants;
187 De, DEX-treated plants; Mo, Mock-treated plants; _4, 4 days of treatment; _12, 12 days of
188 treatment.

189

190 **Fig. S2.** Transcriptomic profiling of dexamethasone (DEX)-treated wild-type Col-0 plants. (a)
191 Morphology of representative wild-type (WT) Arabidopsis plants used for RNA-Seq
192 experiments. Samples were collected after 4 or 12 days of 30 μM DEX treatment and subjected
193 to RNA sequencing. H_2O-treated plants were used as controls. Note that application of DEX
194 has a negative effect on plant growth as deduced by the significant reduction of rosette size
195 after 12 days of DEX treatment relative to the non-treated controls. Box and whisker plot
196 showing 5-95 percentile was analyzed by Mann-Whitney test; ****, p <0.0001. (b) Volcano
197 plots showing the distribution of differentially expressed genes (DEGs) (adjusted p-value ≤
198 0.05). The x-axis shows the gene fold change, and y-axis plots the statistical significance (p-
199 value) of the differences. Significantly up- and down-regulated genes are highlighted in red and
200 green, respectively. Genes that are not differentially regulated are in blue. (c) Principal
201 component analysis (PCA) of RNA-Seq data. The PCA was performed using normalized RNA-
202 Seq data of DEGs between DEX-treated and mock-treated WT plants after 4 and 12 days of
203 treatment (DeWT_vs MoWT_). Each biological replicate is represented in the score plot. The
204 variance explained by each component (%) is given in parentheses. (d) Scatterplot of selected
205 gene ontology (GO) terms of DEGs. GO terms between DEX-treated and mock-treated WT
206 plants at 4 and 12 days of treatment (DeL9_ vs MoL9_) are shown. Dot size represents the
207 count of different genes and the color indicates significance of the term enrichment. GO terms
208 with adjusted p-value < 0.05 are significantly enriched. WT, wild-type Col-0; De, DEX-treated
209 plants; Mo, Mock-treated plants; _4, 4 days of treatment; _12, 12 days of treatment.

210

211 **Fig. S3.** Enrichment analysis of Kyoto Encyclopedia of Genes and Genomes (KEGG) pathways
212 using RNA-Seq data. Scatterplot of selected Kyoto Encyclopedia of Genes and Genomes
213 (KEGG) pathways. Dot size represents the count of different genes and the color indicates
214 significance of the term enrichment. Terms with adjusted p-value < 0.05 are significantly
215 enriched. WT, wild-type Col-0; De, DEX-treated plants; Mo, Mock-treated plants; _4, 4 days
216 of treatment; _12, 12 days of treatment.

217

218 **Fig. S4.** Differential expression of receptor-like protein (RLP)-coding genes in BAK1-
219 INTERACTING RECEPTOR-LIKE KINASE 1 (BIR1) overexpressing plants. (a) Relative
220 expression levels are represented by the number of Fragments Per Kilobase of transcript
221 sequence per Millions of base-pairs sequenced (FPKM) in each of the three independent
222 samples per condition used for RNA-Seq. Significant differences between dexamethasone
223 (DEX)- and mock-treated samples were analyzed using two-way ANOVA followed by Sidak´s
224 multiple comparison test; ***, adjusted *p*-value < 0.001, **< 0.01. Note that the expression
225 levels of each individual replicate within the DEX-treated BIR1 L9_12 group mirror the
226 abundance of BIR1 transcripts in each replicate. (b) Differential expression based on $\log_2$ fold-
227 change in the indicated pairwise comparisons. WT, wild-type Col-0; L9, BIR1 L9 transgenics;
228 De, DEX-treated plants; Mo, mock-treated plants: _4d, 4 days of treatment; _12d, 12 days of
229 treatment.

230

231 **Fig. S5.** Differential expression of cysteine-rich receptor-like kinase (CRK)-coding genes in
232 BAK1-INTERACTING RECEPTOR-LIKE KINASE 1 (BIR1) overexpressing plants. (a)
233 Relative expression levels are represented by the number of Fragments Per Kilobase of
234 transcript sequence per Millions of base-pairs sequenced (FPKM) in each of the three
235 independent samples per condition used for RNA-Seq. Significant differences between
236 dexamethasone (DEX)- and mock-treated samples were analyzed using two-way ANOVA
237 followed by Sidak´s multiple comparison test; ***, adjusted *p*-value < 0.001, **< 0.01. Note
238 that the expression levels of each individual replicate within the DEX-treated BIR1 L9_12
239 group mirror the abundance of BIR1 transcripts in each replicate. (b) Differential expression
240 based on $\log_2$ fold-change in the indicated pairwise comparisons. WT, wild-type Col-0; L9,
241 BIR1 L9 transgenics; De, DEX-treated plants; Mo, mock-treated plants: _4d, 4 days of
242 treatment; _12d, 12 days of treatment.

243

244 **Fig. S6.** Differential expression of cell-surface pattern recognition receptors (PRR)-coding
245 genes in BAK1-INTERACTING RECEPTOR-LIKE KINASE 1 (BIR1) overexpressing plants.
246 Relative expression levels are represented by the number of Fragments Per Kilobase of
247 transcript sequence per Millions of base-pairs sequenced (FPKM) in each of the three
248 independent samples per condition used for RNA-Seq. Significant differences between
249 dexamethasone (DEX)- and mock-treated samples were analyzed using two-way ANOVA

250 followed by Sidak´s multiple comparison test; ***, adjusted *p*-value < 0.001, **< 0.01, *< 0.05.
251 WT, wild-type Col-0; L9, BIR1 L9 transgenics; De, DEX-treated plants; Mo, mock-treated
252 plants: _4d, 4 days of treatment; _12d, 12 days of treatment.

253

254 **Fig. S7**. Differential expression of calcium-dependent protein kinases (CPK)- and
255 HETEROTRIMERIC G PROTEIN-coding genes in BAK1-INTERACTING RECEPTOR-
256 LIKE KINASE 1 (BIR1) overexpressing plants. Relative expression levels are represented by
257 the number of Fragments Per Kilobase of transcript sequence per Millions of base-pairs
258 sequenced (FPKM) in each of the three independent samples per condition used for RNA-Seq.
259 Significant differences between dexamethasone (DEX)- and mock-treated samples were
260 analyzed using two-way ANOVA followed by Sidak´s multiple comparison test; ***, adjusted
261 *p*-value < 0.001, **< 0.01, *< 0.05. WT, wild-type Col-0; L9, BIR1 L9 transgenics; De, DEX-
262 treated plants; Mo, mock-treated plants: _4d, 4 days of treatment; _12d, 12 days of treatment.

263

264 **Fig. S8.** Morphological and growth defects in BAK1-INTERACTING RECEPTOR-LIKE
265 KINASE 1 (BIR1) overexpressing plants of different immune mutant genetic backgrounds. (a)
266 Morphology of transgenic *sobir1-12* BIR1 L8, *bak1-5* BIR1 L4, *eds1*-2 BIR1 L2, *pad4-1* BIR1
267 L12b and *eds5-3* BIR1 L12 mutant plants from independent lines expressing BIR1 under the
268 control of a dexamethasone (DEX)-inducible 35S promoter. Plants were grown for three weeks
269 on soil and treated with 30 µM DEX to activate BIR1 transcription or mock-treated with H_2O.
270 Plants were photographed after 12 days of the first DEX/ H_2O application. (b) Morphology and
271 BIR1 expression levels of DEX- and mock-treated *sobir1-12* BIR1 (L6, L8) and *bak1-5* BIR1
272 (L4, L10) plants as observed in different biological replicates of the experiment. qRT-PCR
273 analysis showed comparable BIR1 transcript levels in both genotypes. Each sample consisted
274 of RNA pooled from six different plants. (c) RT-qPCR analysis of transcripts encoding PTI-
275 marker WRKY DNA-BINDING PROTEIN 29 (WRKY29) in *sobir1-12* BIR1 L6 and *pad4*-1
276 BIR1 L10 mutant backgrounds. In all cases, transcript accumulation was determined in DEX-
277 treated (DEX+) versus mock-treated (DEX-) after 12 days of treatment. Values from
278 biologically independent samples were normalized to the CBP20 internal control, and related
279 to mock-treated plants, set to a value of 1. Data are mean ± SD analyzed by Mann-Whitney test;
280 *, p <0.05. (d) Rosette size (diameter) in wild-type (WT) and BIR1 overexpressing ETI/PTI
281 mutants after 12 days of DEX treatment relative to the non-treated controls. Box and whisker

282 plots showing 5-95 percentile were analyzed by Mann-Whitney test; ****, p <0.0001. Note that
283 rosette size is largely influenced by the effect of DEX on plant development as shown for WT
284 Col-0 plant in this study.

285

286 **Supporting tables**

287 **Table S1**. List of primers

288

289 **Table S2**. List of expressed genes. Values represent the total read counts/ Fragments Per
290 Kilobase of transcript sequence per Millions of base-pairs sequenced (FRKM) values of each
291 biological replicate (a,b,c) per condition and their corresponding row mean values. De (DEX-
292 treated plants), Mo (Mock-treated plants), WT (wild-type plants), L9 (BIR1 L9 transgenic
293 plants), _4 (4 days of treatment), _12 (12 days of treatment)

294

295 **Table S3**. List of differentially expressed genes (DEG. padjust value < 0.05). Values represent
296 the mean Fragments Per Kilobase of transcript sequence per Millions of base-pairs sequenced
297 (FPKM) values from three biological replicates per condition. De (DEX-treated plants), Mo
298 (Mock-treated plants), WT (wild-type plants), L9 (BIR1 L9 transgenic plants), _4 (4 days of
299 treatment), _12 (12 days of treatment).

300

301 **Table S4**. List of differentially expressed genes (DEG. |Log2fold change > 1| padjust value <
302 0.01). Values represent the mean Fragments Per Kilobase of transcript sequence per Millions
303 of base-pairs sequenced (FPKM) values from three biological replicates per condition. De
304 (DEX-treated plants), Mo (Mock-treated plants), WT (wild-type plants), L9 (BIR1 L9
305 transgenic plants), _4 (4 days of treatment), _12 (12 days of treatment).

306

307 **Table S5**. Enrichment analysis of Gene Ontology (GO) terms. CC (cellular component), BP
308 (biological process) and MF (molecular function). Gene Ratio is the ratio of DEGs to all genes
309 for this GO term. Bg Ratio is the ratio of all genes concerning this GO term to all genes in
310 background GO database. Count is the number of differentially expressed genes concerning
311 this GO term. Adjusted p-value < 0.05 means significant enrichment. De (DEX-treated plants),

312 Mo (Mock-treated plants), WT (wild-type plants), L9 (BIR1 L9 transgenic plants), _4 (4 days
313 of treatment), _12 (12 days of treatment).

314

315 **Table S6**. Kyoto Encyclopedia of Genes and Genomes (KEGG) pathway enrichment analysis.
316 Gene Ratio is the ratio of DEGs to all genes for this pathway. Bg Ratio is the ratio of all genes
317 concerning this KEGG term to all genes in background KEGG database. Count is the number
318 of differentially expressed genes concerning this term. Adjusted p-value < 0.05 means
319 significant enrichment. De (DEX-treated plants), Mo (Mock-treated plants), WT (wild-type
320 plants), L9 (BIR1 L9 transgenic plants), _4 (4 days of treatment), _12 (12 days of treatment).

321

322 **Table S7**. List of differentially expressed genes (DEG. padjust value < 0.05) within functional
323 categories. Values represent the mean Fragments Per Kilobase of transcript sequence per
324 Millions of base-pairs sequenced (FPKM) values from three biological replicates per condition.
325 De (DEX-treated plants), Mo (Mock-treated plants), WT (wild-type plants), L9 (BIR1 L9
326 transgenic plants), _4 (4 days of treatment), _12 (12 days of treatment).

327

328 **Table S8**. Statistical analysis of enrichment of functional gene groups in plants overexpressing
329 BIR1 after 12 days of DEX treatment relative to non-expressing controls using Two-tailed
330 Fisher's exact tests. De (DEX-treated plants), Mo (Mock-treated plants), WT (wild-type plants),
331 L9 (BIR1 L9 transgenic plants). LRR, leucine-rich repeat; RLK, receptor-like kinase; CRK,
332 cysteine-rich RLKs; RLP, receptor-like protein; TNL, TIR1-nucleotide-binding domain LRR
333 immune receptors.

334

335

336 **Supporting references**

337

338 **Albert I, Bohm H, Albert M, Feiler CE, Imkampe J, Wallmeroth N, Brancato C,**
339 **Raaymakers TM, Oome S, Zhang H, et al. 2015.** An RLP23-SOBIR1-BAK1 complex
340 mediates NLP-triggered immunity. *Nat Plants* **1**: 15140.

341 **Fernandez-Calvino L, Guzman-Benito I, Del Toro FJ, Donaire L, Castro-Sanz AB, Ruiz-**
342 **Ferrer V, Llave C. 2016.** Activation of senescence-associated Dark-inducible (DIN) genes

343 during infection contributes to enhanced susceptibility to plant viruses. *Mol Plant Pathol*
344 **17**(1): 3-15.
345 **Guzman-Benito I, Donaire L, Amorim-Silva V, Vallarino JG, Esteban A, Wierzbicki AT,**
346 **Ruiz-Ferrer V, Llave C. 2019.** The immune repressor BIR1 contributes to antiviral defense
347 and undergoes transcriptional and post-transcriptional regulation during viral infections.
348 *New Phytol* **224**(1): 421-438.
349 **Huang C, Mutterer J, Heinlein M. 2022.** In Vivo Aniline Blue Staining and Semiautomated
350 Quantification of Callose Deposition at Plasmodesmata. *Methods Mol Biol* **2457**: 151-165.
351 **McNellis TW, Mudgett MB, Li K, Aoyama T, Horvath D, Chua NH, Staskawicz BJ. 1998.**
352 Glucocorticoid-inducible expression of a bacterial avirulence gene in transgenic Arabidopsis
353 induces hypersensitive cell death. *Plant J* **14**(2): 247-257.
354 **Wan WL, Zhang L, Pruitt R, Zaidem M, Brugman R, Ma X, Krol E, Perraki A, Kilian J,**
355 **Grossmann G, et al. 2019.** Comparing Arabidopsis receptor kinase and receptor protein-
356 mediated immune signaling reveals BIK1-dependent differences. *New Phytol* **221**(4): 2080-
357 2095.
358

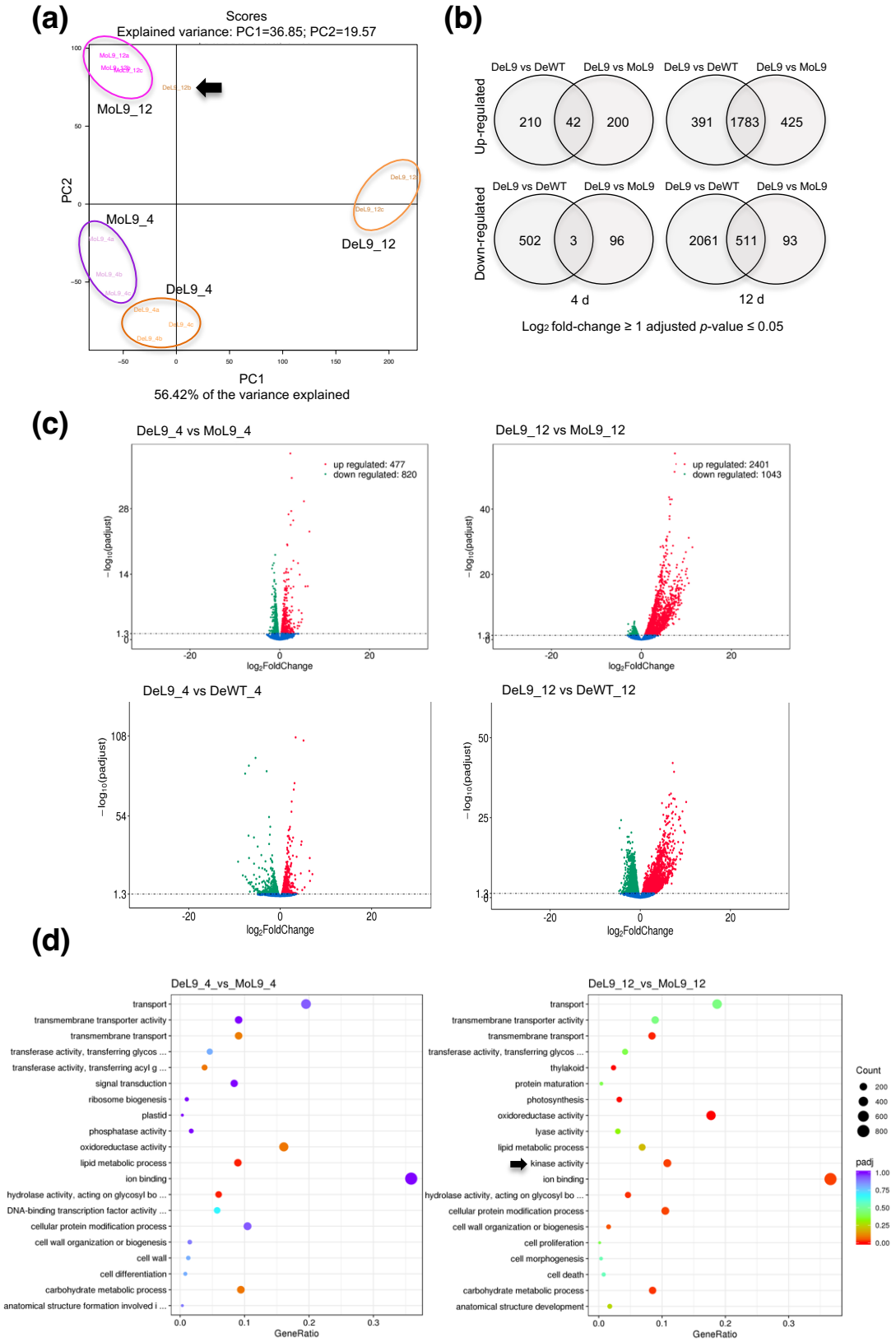

Fig. S1. Transcriptomic profiling of BAK1-INTERACTING RECEPTOR-LIKE KINASE 1 (BIR1) expressing transgenic lines. (a) Principal component analysis (PCA) of RNA-Seq data. The PCA was performed using normalized RNA-Seq data of differentially expressed genes (DEGs) between dexamethasone (DEX)-treated and mock-treated transgenic BIR1 L9 plants after 4 and 12 days of treatment (DeL9_vs MoL9_). Each biological replicate is represented in the score plot. The variance explained by each component (%) is given in parentheses. The sample (DeL9_12b) with differential expression within the DEX-treated L9 group is indicated with a black arrow. (b) Number of up-or down-regulated transcripts, with a $|\log_2(\text{Fold-Change})| \geq 1$ and adjusted *p*-value ≤0.05, in each pairwise comparison as indicated. (c) Volcano plots showing the distribution of DEGs (adjusted *p*-value ≤ 0.05). The x-axis shows the fold change in gene expression between samples, and y-axis shows the statistical significance of the differences. Significantly up- and down-regulated genes are highlighted in red and green, respectively. Genes that are not differentially regulated are in blue. (d) Scatterplot of selected gene ontology (GO) terms of DEGs. GO terms between wild-type (WT) and BIR1 L9 plants at 4 and 12 days after DEX-treatment (DeL9_ vs MoL9_) are shown. Dot size represents the count of different genes and the color indicates significance of the term enrichment. GO terms with adjusted *p*-value < 0.05 are significantly enriched. The kinase term (indicated by an arrow) was exclusively assigned to BIR1 L9 plants. WT, wild-type Col-0; L9, BIR1 L9 transgenic plants; De, DEX-treated plants; Mo, Mock-treated plants; _4, 4 days of treatment; _12, 12 days of treatment.

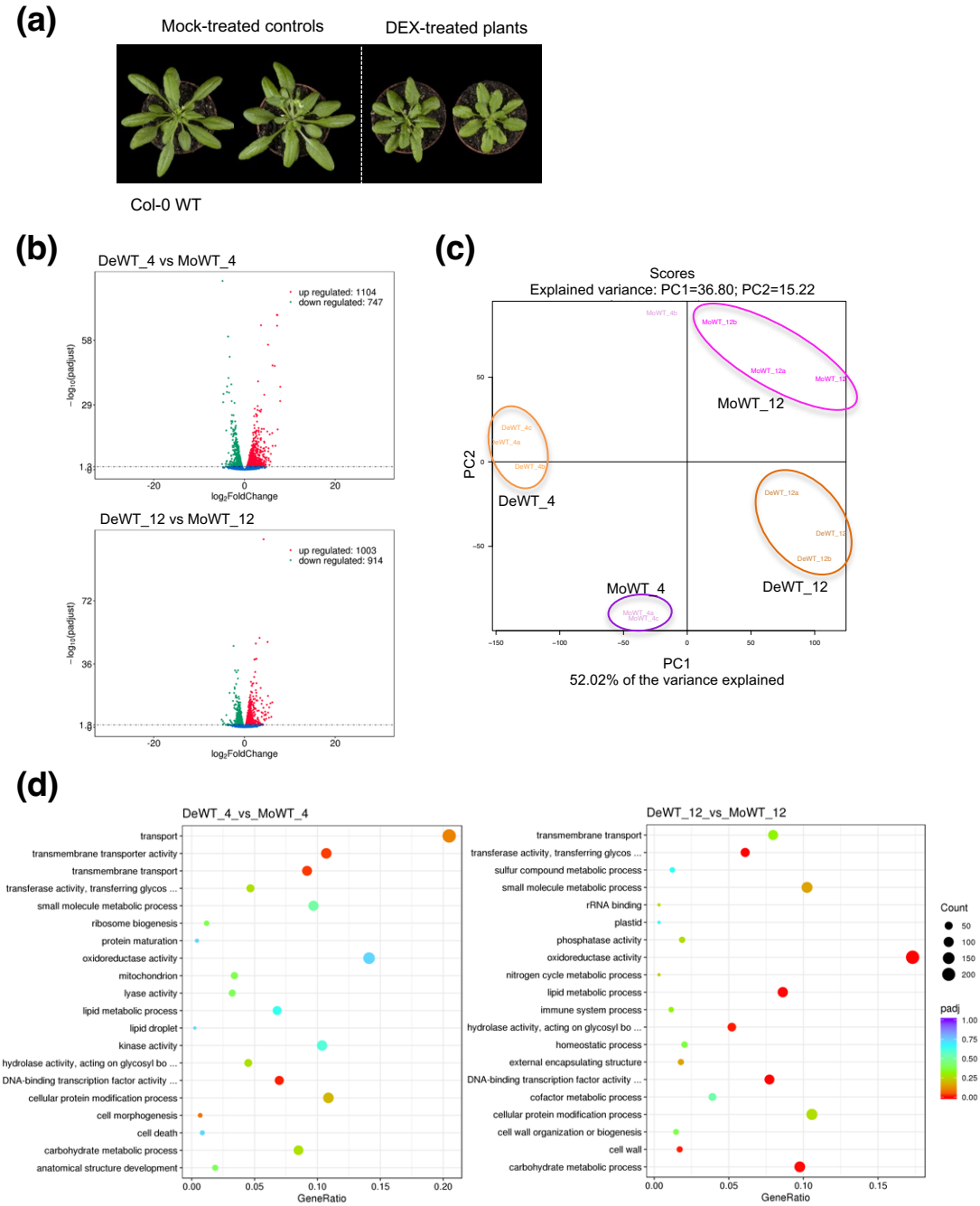

Fig. S2. Transcriptomic profiling of dexamethasone (DEX)-treated wild-type Col-0 plants. (a) Morphology of representative wild-type (WT) Arabidopsis plants used for RNA-Seq experiments. Samples were collected after 4 or 12 days of 30 μM DEX treatment and subjected to RNA sequencing. H_2O-treated plants were used as controls. Note that application of DEX has a negative effect on plant growth as deduced by the significant reduction of rosette size after 12 days of DEX treatment relative to the non-treated controls. Box and whisker plot showing 5-95 percentile was analyzed by Mann-Whitney test; ****, $p < 0.0001$. (b) Volcano plots showing the distribution of differentially expressed genes (DEGs) (adjusted p-value ≤ 0.05). The x-axis shows the gene fold change, and y-axis plots the statistical significance (p-value) of the differences. Significantly up- and down-regulated genes are highlighted in red and green, respectively. Genes that are not differentially regulated are in blue. (c) Principal component analysis (PCA) of RNA-Seq data. The PCA was performed using normalized RNA-Seq data of DEGs between DEX-treated and mock-treated WT plants after 4 and 12 days of treatment (DeWT_vs MoWT_). Each biological replicate is represented in the score plot. The variance explained by each component (%) is given in parentheses. (d) Scatterplot of selected gene ontology (GO) terms of DEGs. GO terms between DEX-treated and mock-treated WT plants at 4 and 12 days of treatment (DeL9_ vs MoL9_) are shown. Dot size represents the count of different genes and the color indicates significance of the term enrichment. GO terms with adjusted p-value < 0.05 are significantly enriched. WT, wild-type Col-0; De, DEX-treated plants; Mo, Mock-treated plants; _4, 4 days of treatment; _12, 12 days of treatment.

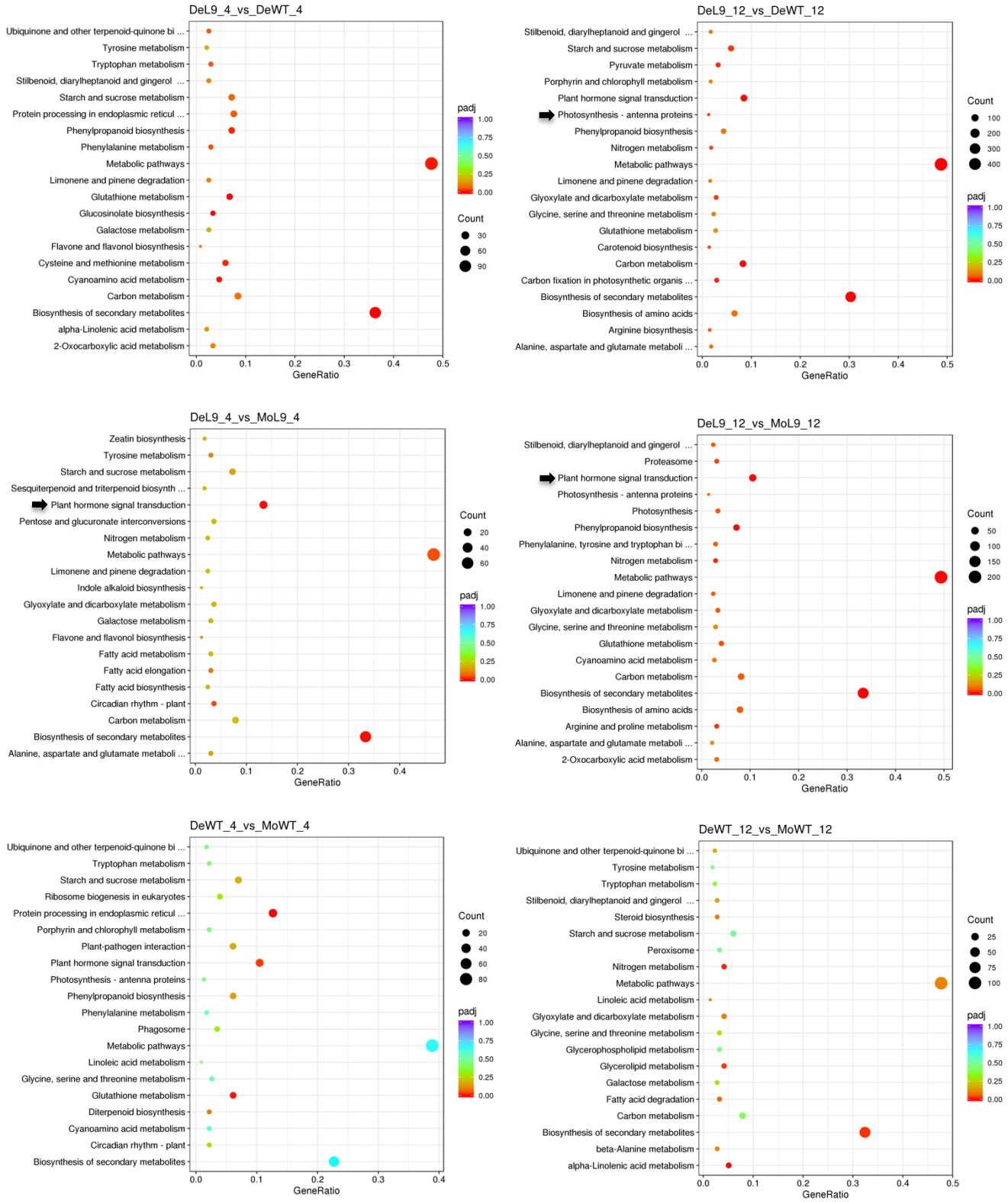

Fig. S3. Enrichment analysis of Kyoto Encyclopedia of Genes and Genomes (KEGG) pathways using RNA-Seq data. Scatterplot of selected Kyoto Encyclopedia of Genes and Genomes (KEGG) pathways. Dot size represents the count of different genes and the color indicates significance of the term enrichment. Terms with adjusted p-value < 0.05 are significantly enriched. WT, wild-type Col-0; De, DEX-treated plants; Mo, Mock-treated plants; _4, 4 days of treatment; _12, 12 days of treatment.

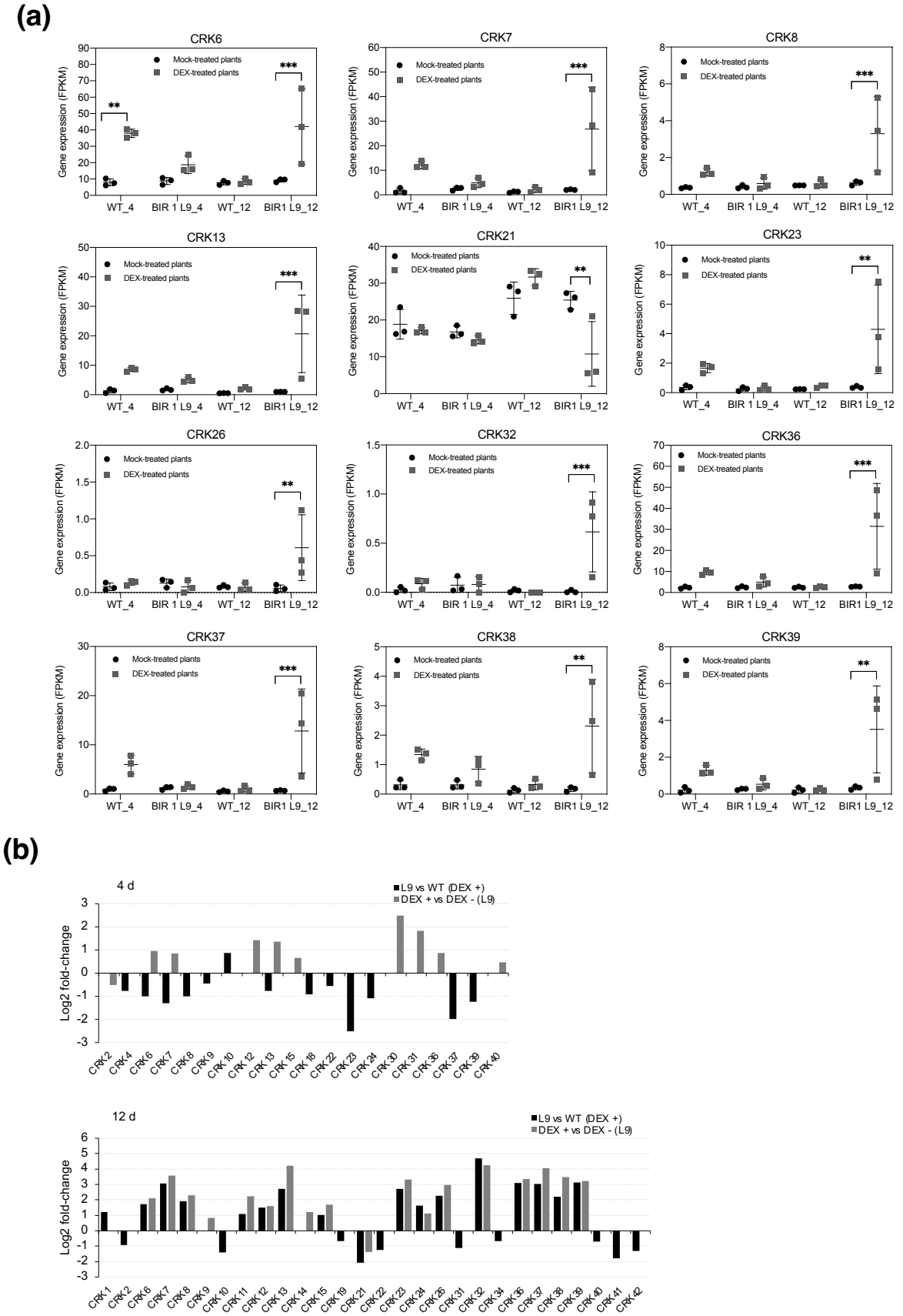

Fig. S4. Differential expression of receptor-like protein (RLP)-coding genes in BAK1-INTERACTING RECEPTOR-LIKE KINASE 1 (BIR1) overexpressing plants. (a) Relative expression levels are represented by the number of Fragments Per Kilobase of transcript sequence per Millions of base-pairs sequenced (FPKM) in each of the three independent samples per condition used for RNA-Seq. Significant differences between dexamethasone (DEX)- and mock-treated samples were analyzed using two-way ANOVA followed by Sidak´s multiple comparison test; ***, adjusted *p*-value < 0.001, **< 0.01. Note that the expression levels of each individual replicate within the DEX-treated BIR1 L9_12 group mirror the abundance of BIR1 transcripts in each replicate. (b) Differential expression based on $\log_2$ fold-change in the indicated pairwise comparisons. WT, wild-type Col-0; L9, BIR1 L9 transgenics; De, DEX-treated plants; Mo, mock-treated plants: _4d, 4 days of treatment; _12d, 12 days of treatment.

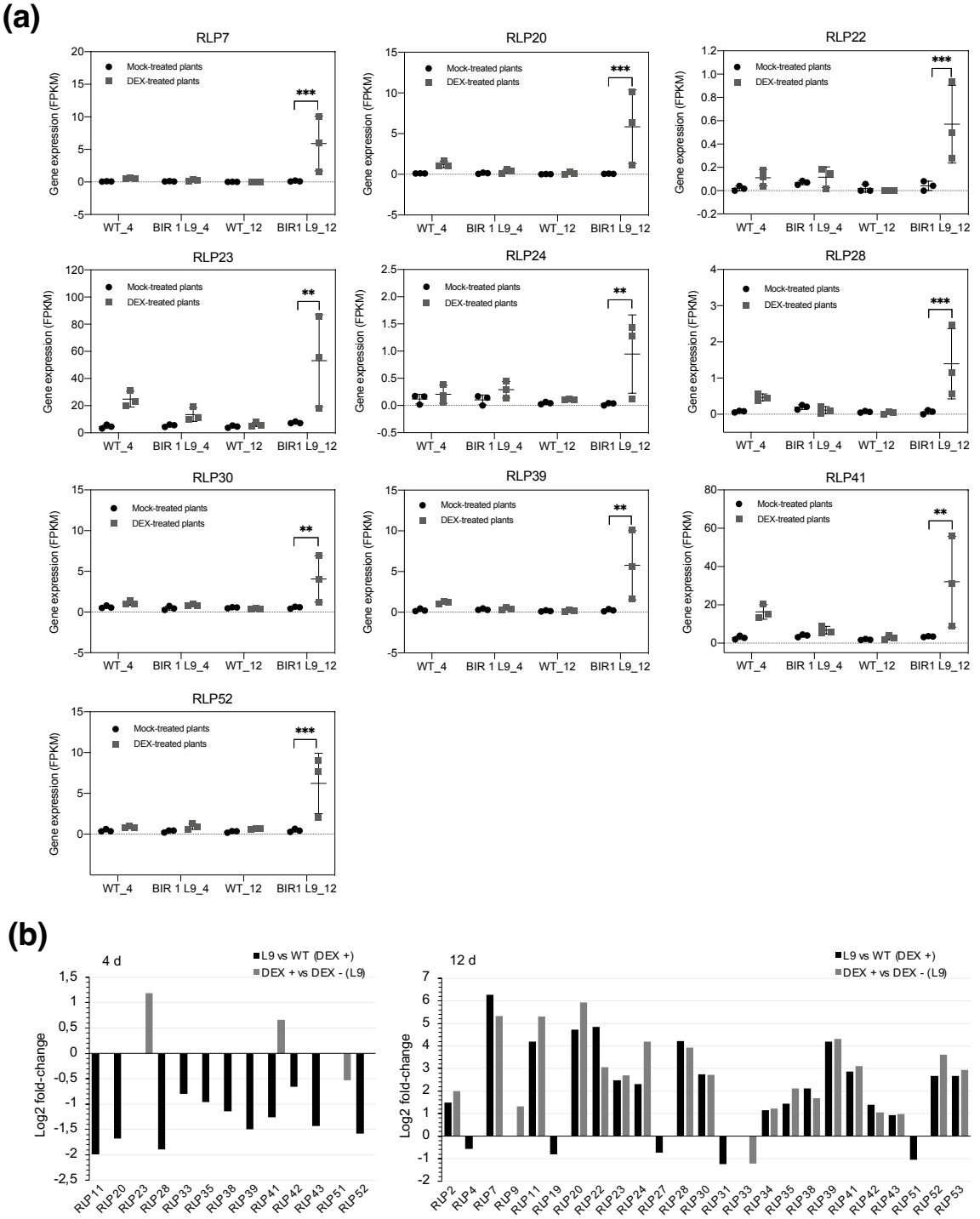

Fig. S5. Differential expression of cysteine-rich receptor-like kinase (CRK)-coding genes in BAK1-INTERACTING RECEPTOR-LIKE KINASE 1 (BIR1) overexpressing plants. (a) Relative expression levels are represented by the number of Fragments Per Kilobase of transcript sequence per Millions of base-pairs sequenced (FPKM) in each of the three independent samples per condition used for RNA-Seq. Significant differences between dexamethasone (DEX)- and mock-treated samples were analyzed using two-way ANOVA followed by Sidak´s multiple comparison test; ***, adjusted *p*-value < 0.001, **< 0.01. Note that the expression levels of each individual replicate within the DEX-treated BIR1 L9_12 group mirror the abundance of BIR1 transcripts in each replicate. (b) Differential expression based on $\log_2$ fold-change in the indicated pairwise comparisons. WT, wild-type Col-0; L9, BIR1 L9 transgenics; De, DEX-treated plants; Mo, mock-treated plants: _4d, 4 days of treatment; _12d, 12 days of treatment.

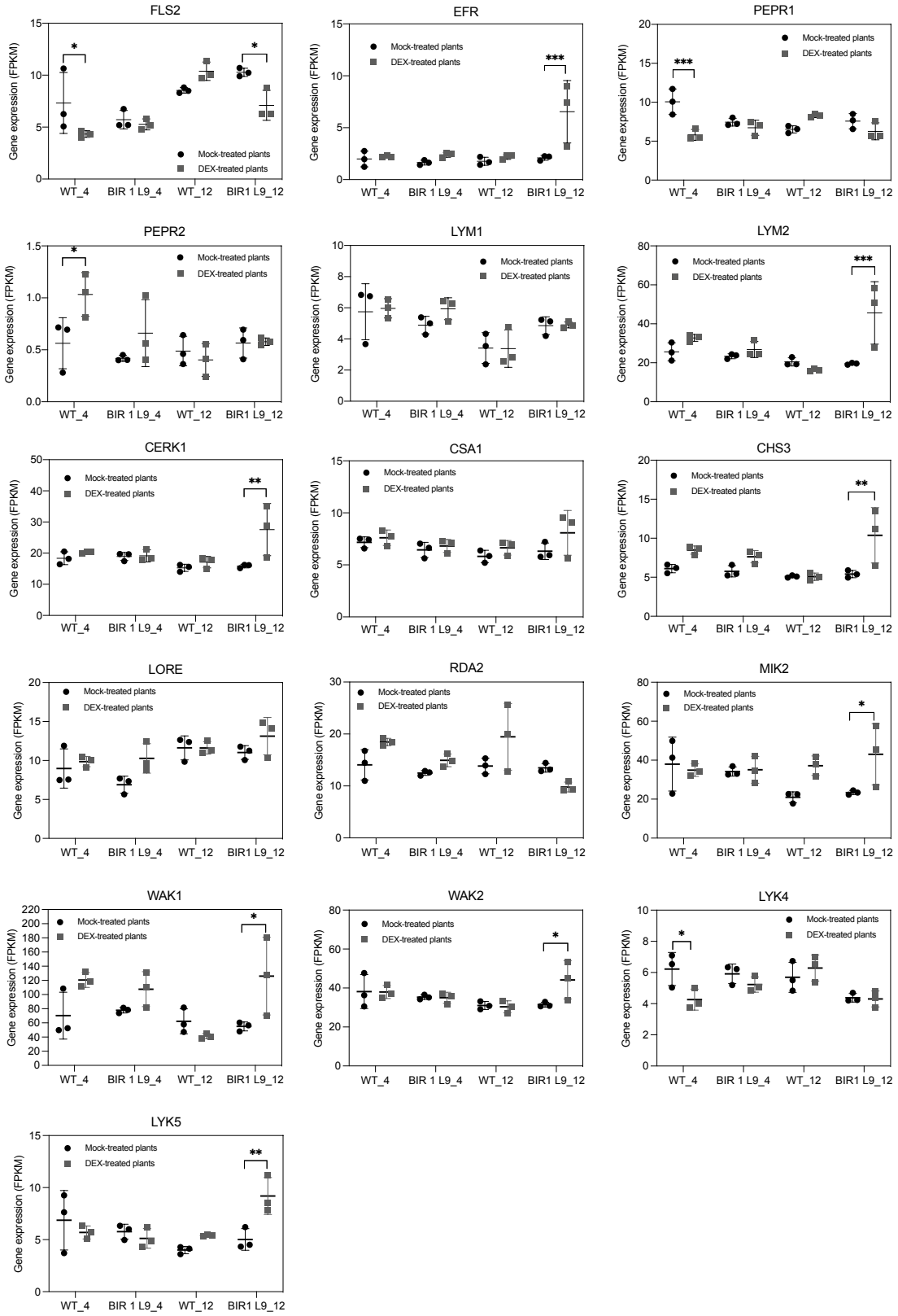

Fig. S6. Differential expression of cell-surface pattern recognition receptors (PRR)-coding genes in BAK1-INTERACTING RECEPTOR-LIKE KINASE 1 (BIR1) overexpressing plants. Relative expression levels are represented by the number of Fragments Per Kilobase of transcript sequence per Millions of base-pairs sequenced (FPKM) in each of the three independent samples per condition used for RNA-Seq. Significant differences between dexamethasone (DEX)- and mock-treated samples were analyzed using two-way ANOVA followed by Sidak´s multiple comparison test; ***, adjusted *p*-value < 0.001, **< 0.01, *< 0.05. WT, wild-type Col-0; L9, BIR1 L9 transgenics; De, DEX-treated plants; Mo, mock-treated plants: _4d, 4 days of treatment; _12d, 12 days of treatment.

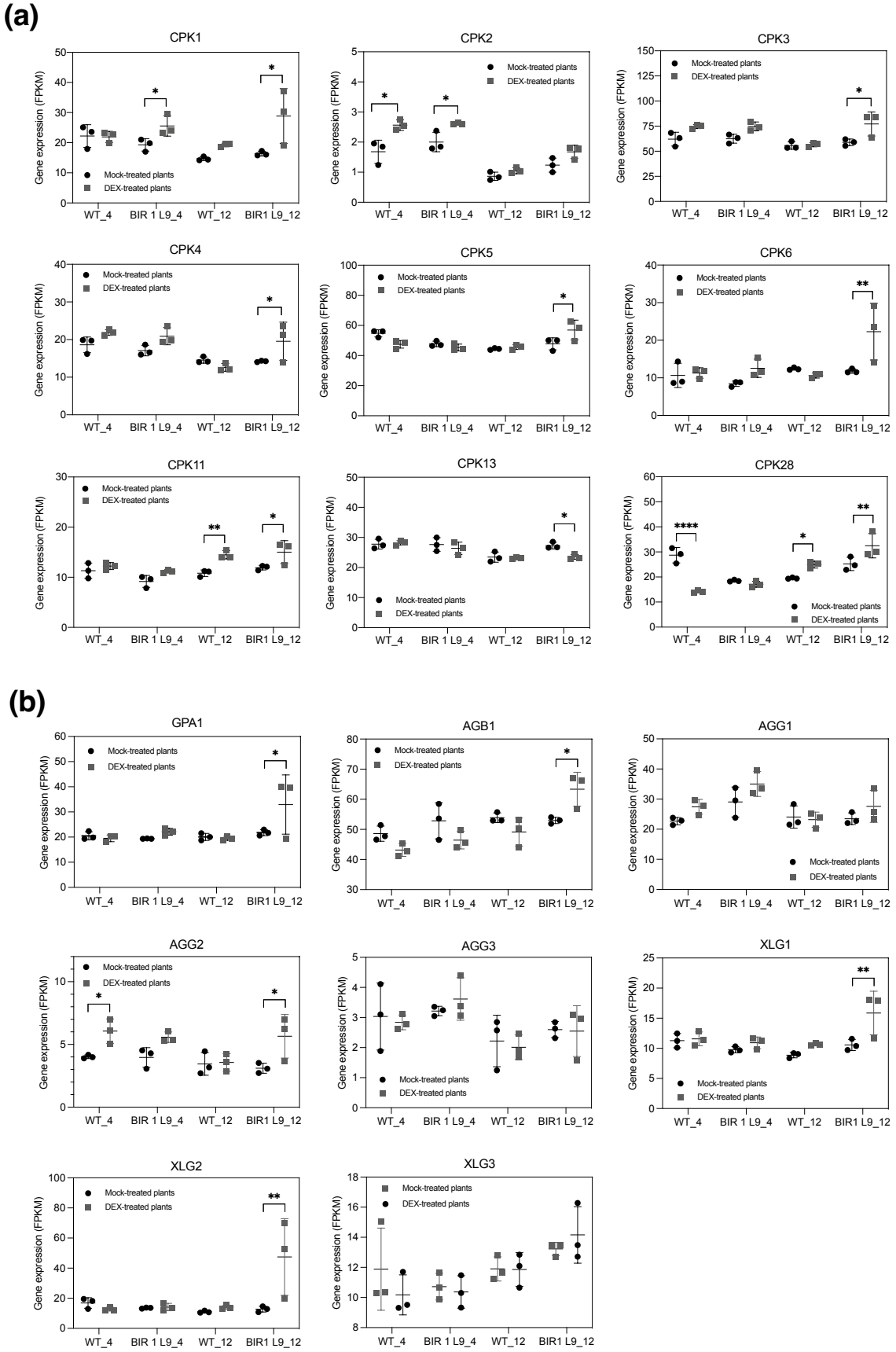

Fig. S7. Differential expression of calcium-dependent protein kinases (CPK)- and HETEROTRIMERIC G PROTEIN-coding genes in BAK1-INTERACTING RECEPTOR-LIKE KINASE 1 (BIR1) overexpressing plants. Relative expression levels are represented by the number of Fragments Per Kilobase of transcript sequence per Millions of base-pairs sequenced (FPKM) in each of the three independent samples per condition used for RNA-Seq. Significant differences between dexamethasone (DEX)- and mock-treated samples were analyzed using two-way ANOVA followed by Sidak´s multiple comparison test; ***, adjusted *p*-value < 0.001, **< 0.01, *< 0.05. WT, wild-type Col-0; L9, BIR1 L9 transgenics; De, DEX-treated plants; Mo, mock-treated plants: _4d, 4 days of treatment; _12d, 12 days of treatment.

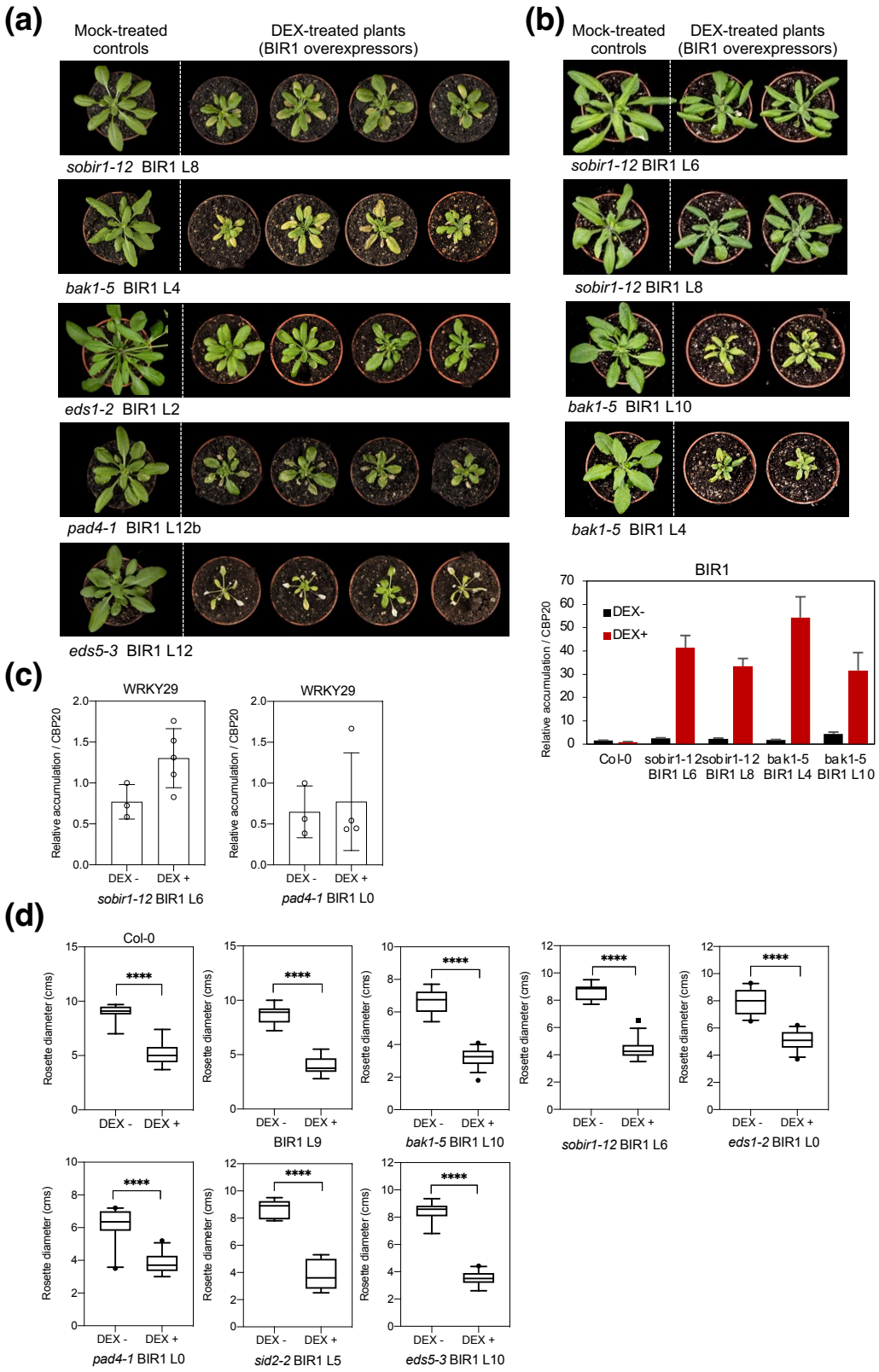

Fig. S8. Morphological and growth defects in BAK1-INTERACTING RECEPTOR-LIKE KINASE 1 (BIR1) overexpressing plants of different immune mutant genetic backgrounds. (a) Morphology of transgenic *sobir1-12* BIR1 L8, *bak1-5* BIR1 L4, *eds1-2* BIR1 L2, *pad4-1* BIR1 L12b and *eds5-3* BIR1 L12 mutant plants from independent lines expressing BIR1 under the control of a dexamethasone (DEX)-inducible 35S promoter. Plants were grown for three weeks on soil and treated with 30 µM DEX to activate BIR1 transcription or mock-treated with H_2O. Plants were photographed after 12 days of the first DEX/ H_2O application. (b) Morphology and BIR1 expression levels of DEX- and mock-treated *sobir1-12* BIR1 (L6, L8) and *bak1-5* BIR1 (L4, L10) plants as observed in different biological replicates of the experiment. qRT-PCR analysis showed comparable BIR1 transcript levels in both genotypes. Each sample consisted of RNA pooled from six different plants. (c) RT-qPCR analysis of transcripts encoding PTI-marker WRKY DNA-BINDING PROTEIN 29 (WRKY29) in *sobir1-12* BIR1 L6 and *pad4*-1 BIR1 L10 mutant backgrounds. In all cases, transcript accumulation was determined in DEX-treated (DEX+) versus mock-treated (DEX-) after 12 days of treatment. Values from biologically independent samples were normalized to the CBP20 internal control, and related to mock-treated plants, set to a value of 1. Data are mean ± SD analyzed by Mann-Whitney test; *, $p < 0.05$. (d) Rosette size (diameter) in wild-type (WT) and BIR1 overexpressing ETI/PTI mutants after 12 days of DEX treatment relative to the non-treated controls. Box and whisker plots showing 5-95 percentile were analyzed by Mann-Whitney test; ****, $p < 0.0001$. Note that rosette size is largely influenced by the effect of DEX on plant development as shown for WT Col-0 plant in this study.